International Journal of Heat and Mass Transfer 194 (2022) 123069

Contents lists available at ScienceDirect

International Journal of Heat and Mass Transfer

journal homepage: www.elsevier.com/locate/hmt

Improved correlation for heat transfer during condensation in mini and macro channels

Mirza M. Shah

Engineering Research Associates, Redding, CT 06896, United States

ARTICLE INFO

Article history:
Received 9 February 2022
Revised 16 May 2022
Accepted 21 May 2022

Keywords:
Condensation
Heat transfer
Mini-channels
Macro-channels
Correlation

ABSTRACT

An improved version of the present author's earlier correlation for heat transfer during condensation in conventional and mini channels is presented. It has been validated by comparison with a database that includes 51 fluids (water, refrigerants, chemicals, cryogens), diameters 0.08 to 49.0 mm, reduced pressures 0.0006 to 0.949, mass flux from 1.1 to 1400 $kgm^{-2}s^{-1}$, various shapes (round, rectangular, triangular, etc.), single and multi-channels, annuli, horizontal and vertical downflow. The data are from 130 sources. The improved correlation predicts 8298 data points with mean absolute deviation (MAD) of 17.9 %. The same data are also compared to other correlations. Their deviations are much greater.

1. Introduction

Condensation of vapors is involved in many industries including refrigeration, conventional and nuclear power plants, chemical processing, etc. In the past, most condensers used comparatively large diameter round tubes. In recent years, there has been increasing use of small diameter channels of various shapes as these provide higher heat transfer coefficients and occupy less space. They also reduce the amount of refrigerant in refrigeration systems and thus minimize environmental impact in case of leakage. Hence methods for predicting heat transfer are needed for conventional (macro) tube sizes as well as mini/micro channels. Many correlations have been published for this purpose. The present author published a correlation, Shah [154], which gave good agreement with wide ranging data from 88 sources. Since then, several new refrigerants have been introduced and much more test data has been published. Several new correlations have also been published. It was therefore felt desirable to compare the new and previous correlations to new data to ascertain their accuracy. A project was therefore undertaken for this purpose. A very large database consisting of new as well as previously analyzed data was compared to leading published correlations. During this work, an improved correlation was developed by modifying the author's earlier correlation, Shah [154].

In the following, the previous research in this field is discussed, the development of the improved correlation is described, and its comparison with a wide-ranging database is presented. The database includes 51 fluids (water, natural refrigerants CO_2 and ammonia, various types of halocarbon refrigerants, hydrocarbons, cryogen nitrogen, heat transfer fluids), diameters 0.08 to 49.0 mm, reduced pressures 0.0006 to 0.946, mass flux from 1.1 to 1400 kg $m^{-2}s^{-1}$, various shapes (round, rectangular, triangular, etc.), horizontal and vertical downflow. The improved correlation predicts 8298 data points from 130 sources with mean absolute deviation (MAD) of 17.9 %. The same data were also compared to other leading correlations. They had considerably larger deviations. A simple criterion is given for the range of reasonable accuracy of the Shah [141] correlation in view of its wide use in analyzes such as heat recovery and bottoming cycles.

Note that all discussions in this paper pertain to plain channels. Channels with fins or other enhancement devices are not considered.

2. Previous work

There have been many published experimental studies on heat transfer during condensation in tubes over the last hundred years. The studies in recent years have predominantly been on minichannels. Many predictive methods, theoretical and empirical have been proposed, starting with the laminar flow analysis by Nusselt. The experimental work and prediction methods have been most recently reviewed by Shah [156]. Earlier reviews include Collier and Thome [40], Del Col et al. [47], Zhang et al. [184], and Riefert et al. [137]. These researches will be briefly reviewed in the following. Before doing so, it is desirable to briefly discuss the boundary between mini and macro channels.

E-mail address: mshah.erc@gmail.com

https://doi.org/10.1016/j.ijheatmasstransfer.2022.123069
0017-9310/

Nomenclature

AD	average deviation, (-)
Bo	bond number = $g(\rho_L - \rho_G)D^2 \sigma^{-1}$, (-)
C_{pg}	specific heat of vapor at constant pressure, J $kg^{-1}K^{-1}$
D	inside diameter of tube, m
D_{HP}	equivalent diameter based on perimeter with heat transfer, defined by Eq. (16), m
D_{HYD}	hydraulic equivalent diameter defined by Eq. (17), m
Fr_{LT}	froude number $=G^2\rho_L{}^{-2}g^{-1}D^{-1}$, (-)
G	total mass flux (liquid + vapor), kg $m^{-2}s^{-1}$
g	acceleration due to gravity, m s^{-2}
h	heat transfer coefficient, W m^{-2} K^{-1}
h_I	heat transfer coefficient given by Eq. (2), W m^{-2} K^{-1}
h_{GS}	heat transfer coefficient assuming vapor phase flowing alone in the tube, Wm^{-2} K^{-1}
h_{LS}	heat transfer coefficient assuming liquid phase flowing alone in the tube, Wm^{-2} K^{-1}
h_{LT}	heat transfer coefficient with total mass flowing as liquid, W m^{-2} K^{-1}
h_{Nu}	heat transfer coefficient given by Eq.(3), the Nusselt equation, W m^{-2} K^{-1}
h_{TP}	two-phase heat transfer coefficient, W m^{-2} K^{-1}
J_g	dimensionless vapor velocity defined by Eq. (11)
k	thermal conductivity, W m^{-1} K^{-1}
MAD	mean absolute deviation, (-)
N	number of data points, (-)
p_r	reduced pressure, (-)
Pr	prandtl number, (-)
Re_{GT}	Reynolds number for all mass flowing as vapor = $GD\mu_G{}^{-1}$, (-)
Re_{LS}	Reynolds number assuming liquid phase flowing alone, = $G(1 - x)D\mu_L{}^{-1}$, (-)
Re_{LT}	Reynolds number for all mass flowing as liquid = $GD\mu_L{}^{-1}$, (-)
T	temperature, K
T_{BP}	bubble point of mixture, K
T_{DP}	dew point of temperature, K
T_{glide}	$(T_{DP} - T_{BP})$, K
T_{SAT}	saturation temperature, °C
T_w	wall temperature, °C
ΔT	$= (T_{SAT} - T_W)$, K
We_{GT}	weber number for all mass flowing as vapor, defined by Eq. (14), (-)
x	vapor quality, (-)
Z	shah's correlating parameter defined by Eq. (8), (-)

Greek

μ	dynamic viscosity, Pa. s
ρ	density, kg m^{-3}
Σ	mathematical symbol for summation
σ	surface tension, Nm^{-1}

Subscripts

G	vapor
L	liquid

2.1. Boundary between mini and macro channels

The most widely used classification is that by Kandlikar [85]. According to it, channels with D_{HYD} > 3 mm are macro (conventional) while those with $D_{HYD} \leq 3$ mm are mini/micro channels. This is a physical dimension criterion. Many researchers consider the regime of minichannels to start when surface tension begins to have effect and correlations for macro channels begin to fail due to it. Many of these classifications use Bond number or its equivalent confinement and Eotvos numbers to define the boundary. Shah [151] evaluated these classifications against data for boiling, condensation, and two-component flow in channels. He found that none of them is able to predict the limit of applicability of heat transfer correlations for conventional channels to mini channels.

As the classification of Kandlikar is in wide use, channels with $D_{HYD} \leq 3$ mm are called minichannels in this paper.

2.2. Experimental studies

There have been numerous experimental studies in which heat transfer coefficients in channels were measured. Some of them do not provide sufficient details for comparing them to prediction methods. In Shah [154] data from 88 experimental studies were analyzed. The salient features of those experimental studies are given in Shah [147,148,154] and are summarized in Table 1 . These include both mini and macro channels. The papers by Dorao and Fernandino [57] and Kim and Mudawar [93] list many experimental studies. Thirty-six more experimental studies which provide analyzable data were identified during the present research. They are listed in Table 2 along with their features. These include data for a number of new refrigerants as well as for nitrogen. The new data also include two studies using annuli while those mentioned above did not have any data for annuli.

2.3. Prediction methods

2.3.1. Analytical approaches

A number of early authors analyzed a symmetrical annular flow pattern assuming that the velocity profile in the liquid layer is similar to that in single phase flow or assuming that the eddy diffusivity distribution is similar to that in single phase flow. Various other assumptions and simplifications were also made. Most authors solved the resulting equations numerically and presented the results in the form of graphs or equations fitted to the computer output. A few solved the equations analytically with more simplifying assumptions and came up with design equations. Among these, that of Traviss et al. [167] has been quoted extensively and is compared to test data in the present research.

Many other analyzes of condensation in annular and other flow patterns have been done, most of them numerically. These include many CFD simulations. These efforts have been reviewed among others by Kharangate and Mudawar (2017) and Keniar et al. [88]. None of the published studies have been shown to agree with varied data from many sources. While these analyzes have increased our understanding of the phenomena, they are as yet not suitable for use in design.

2.3.2. Correlations

A very large number of correlations have been proposed. The vast majority of them are based only on the authors' own test data. A few correlations have been developed using data from many sources for many fluids and covering a wide range of parameters. Only such correlations are discussed here.

Some correlations are based on flow patterns. Among those are the correlations of Thome et al. (2003) and Shah [146]. The latter was shown to be in good agreement with data for 25 fluids in horizontal tubes of 2 to 49 mm diameter. The difficulty in using flow pattern-based correlations is the unavailability of accurate flow pattern maps. As discussed in Shah [156], many authors have reported wide discrepancies of their flow pattern data with published flow pattern maps.

Table 1
Range of data which were analyzed in Shah [154]. These were also analyzed in the present study.

Source	Geometry	$D_{hyd}(D_{HP})$mm	Fluid	p_r	GKg. $m^{-2}s^{-1}$	Source	Geometry	$D_{hyd}(D_{HP})$mm	Fluid	p_r	GKg. $m^{-2}s^{-1}$
Belchi et al. [23]	Multi, square, H	1.16	Propane	0.2529 0.4017	175 350	Del Col et al. [46]	Round tube V	1.23	R-134a, R-32	0.249 0.427	100 390
Fries et al. [62, 63]	Round tube, H	20.8 14.5	Isobutane	0.1255 0.1741	150 400	Meyer et al. [119]	Round tube V	8.34	R-134a	0.189 0.323	200 400
Azzolin et al. [14]	Round tube, H	3.4	HFE-7000	0.0181	75 130	Xing et al. [181]	Round tube V	14.81	R-245fa	0.110	199 699
Li et al. [108]	Round tube, H	4.73	CO_2	0.3575 0.4705	100 500	Blangetti and Schlunder [26]	Round tube V	30.0	Water, Dowtherm 209	0.0046 0.008	3.8 81
Guo et al. [71]	Round tube, H	2.0	R-1234ze, R-134a, R-41,R-32,propame,R-161	0.1828 0.8146	200 400	Al-Shammari [6]	Round tube V	28.2	Water	0.0008	3.0
Garimella et al. [66]	Rect., multi, H	0.10 0.16	R-134a	0.1889 0.4128	300 800	Jakob et al. [79]	Round tube V	40.0	Water	0.0046	24 48
Yu et al [183]	Round tube, curved, H	10.0	R-32	0.2125 0.3607	224 394	Kuhn et al. [98]	Round tube V	47.5	Water	0.0227	9.6
Aroonrat and Wongwises [12]	Round tube, H	8.1	R-134a	0.2494	400	Borishanskiy et al. [29]	Round tube V	10.0 20.0	Water	0.036 0.308	12 451
Del Col et al. [49]	Round tube, H	0.96	R-270 (propylene)	0.3607	82 800	Lee and Kim [102]	Round tube V	12.0	Water	0.0046	27 45
Nakashita [127]	Multi, Rect., H	0.76 1.06	R-134a	0.4128	100 400	Goodykoontz and Dorsch [70]	Round tube V	7.44	Water	0.002 0.0065	131 265
Jige et al. [82]	Multi, 0.66 × 0.95 mm, H	0.85 (0.85)	R-1234ze, R-32, R-134a	0.210 0.678	100 400	Carpenter [30]	Round tube V	11.6	Ethanol, toluene, methanol, water	0.0049 0.0583	11 154
Rahman et al. [136]	Multi, rect., H	0.81 (0.81)	R-134a	0.2176	50 200	Murphy [126]	Round tube V	1.93	Propane	0.376 0.656	75 150
Baird et al. [19]	Round tube, H	0.92 1.95	R-123	0.0394 0.1059	170 550	Lilburne and Wood [110]	Round tube V	34.7	R-113	0.0301 0.0343	18 50
Andresen [10]	Round tube, H	0.76 3.05	R-410A	0.8 0.9	200 800	Cavallini and Zecchin [33]	Round tube V	20.0	R-11	0.0249 0.0290	85 303
Mitra [122]	Round tube, H	6.2 9.4	R-410A	0.8 0.9	300 700	Mochizugi et al. [123]	Round tube V	13.9	R-11	0.0424	80
Nie et al. [129]	Round tube, H	19.0	Water	0.1808 0.4523	800	Matkovic et al. [114]	Round H	0.96	R-32, R-134a	0.249 0.429	100 1200
Kim et al. [93]	Round tube, H	5.0	R-410A	0.5542	100 400	Cavallini et al. [38]	Round H	0.80	R-134a	0.256	800
Aprea et al. [11]	Round tube, H	20.0	R-22	0.2805 0.3032	45 120	Del Col et al. [44]	Square H	1.23	R-134a	0.249	200 789
Ghim et al. [68]	Round tube, H	7.75	R-245fa, pentane	0.0924	100 700	Del Col et al. [46]	Square H	1.23	R-32	0.427	100 390
Ghim et al. [69]	Round tube, H	7.75	HFE-7000, Novec 649	0.093 0.094	150 500	Del Col et al. [45,48]	Round H	0.96	Propane, R-1234ze	0.21 0.321	100 800
Fronk and Garimella [65]	Round tube, H	0.98 2.16	Ammonia	0.1788 0.230	75 250	Liu et al. [111]	Square Round H	0.952 1.152	R-152a	0.200	200 800
Zhuang et al. [186]	Round tube, H	4.0	Ethane	0.2105 0.5236	100 257	Derby et al. [51]	Square semi-circle, triang.H	1.0 1.64 (1 to 1.33)	R-134a	0.218 0.285	75 450
Zhuang et al. [187]	Round tube, H	4.0	Me-thane	0.4327 0.7569	99 255	Shin and Kim [159]	Square Round H	0.4941.067	R-134a	0.25	100 600
Li et al. [107]	Single & multi round, H	0.86 4.73	CO_2, R-32, R-134a	0.2176 0.4705	100 500	Wen et al. [177]	Round H	2.46	Butane, R-134a, propane	0.10 0.32	205 510
Dong and Yang [56]	Multi, rect, H	0.067 0.114 (0.133 0.144)	R-141b	0.0449	200	[75]	Round H	1.6	R410A	0.492	500 600

(continued on next page)

Table 1 (*continued*)

Source	Geometry	$D_{hyd}(D_{HP})$mm	Fluid	p_r	GKg. $m^{-2}s^{-1}$	Source	Geometry	$D_{hyd}(D_{HP})$mm	Fluid	p_r	GKg. $m^{-2}s^{-1}$
Al-Zaidi [8]	Multi, rect. 0.4 × 1.0	0.57 (0.67)	HFE-7100	0.0455	48 126	Derby et al. [50]	Multi Round	1.0 (1.33)	R-134a	0.285	257
Meyer and Ewim. [120]	Round tube, H	8.38	R-134a	0.2494	50 200	Cavallini et al. [36]	13 chan. 1.4 × 1.4 mm	1.4	R-410A	0.492	200 1400
Ghorbani et al. [189]	Round tube, H	8.7	Isobutane	0.1458	110 372	Agarwal et al. [2]	Square, 17 chan.	0.762	R-134a	0.166	150 750
Keinath and Garimella [87]	Round tube, H	0.86 3.05	R-404A	0.3799 0.6136	200 800	Bandhauer, et al. [22]	Multi, Round	0.506 1.52	R-134a	0.32	300 750
Liu et al. (2016)	Round & sq. tubes, H	0.952 1.085	R-1234ze, propane, R-22	0.2733 0.4017	200 800	Kim and Mudawar [90]	Multi	1.0 (1.33)	FC-72	0.057	68 367
Del Col et al. [45,46]	Round tube, H	0.96	Propane	0.32	100 800	Vardhan [168]	Multi, circular	1.49	R-134a, R-22	0.338 0.404	434 1084
Murphy [126]	Round tube, V	1.93	Propane	0.3761 0.6556	75 125	Huai and Koyama [74]	Multi, round	1.31	CO2	0.877 0.942	126 241
Varma [169]	Round tube, H	49.0	Water	0.0023	12.6	Fronk and Garimella [64]	Multi, square	0.100	CO2	0.687 0.774	600
Wang & Du [172]	Round tube, H, V	1.98 4.98	Water	0.0055	11 94	Yan and Lin [182]	Multi, round	2.0	R-134a	0.16 0.32	100 200
Borishanski et al. [29]	Round tube, V	20.0	Water	0.1321	6.5 451	Koyama et al. [96]	Multi Rect..	0.807	R-134a	0.418	273 652
Blangetti and Schlunder [26,27]	Round tube, V	30.0	Water, dowtherm	0.0046 0.008	3.8 81	Al-Hajri et al. [4]	0.4 × 2.8 mm	0.7	R245fa, R-134a	0.048 0.168	50 500
Dobson et al. [54]	Round, H	3.14 7.04	R-22, R-134a	0.212 0.349	26 800	Eckels et al. [58]	Round, H	8.0 11.1	R-12, R-134a	0.231 0.244	87 374
Milke [121]	Round, H	7.75	R-245fa, pentane	0.0332 0.1663	100 600	Dobson and Chato [55]	Round, H	7.04	R-410A	0.435	75 650
Macdonald [112]	Round, H	7.5 14.45	Propane	0.253 0.949	150 454	Wijaya and Spatz [178]	Round, H	7.75	R-410A, R-22	0.270 0.647	481 495
Tepe and Mueller [164]	Round, H, V	18.5	Benzene	0.021	52 88	Meyer et al. [119]	Round, H	8.34	R-134a	0.189 0.323	100 400
Azer et al. [13]	Round, H	12.7	R-12	0.218 0.293	231 446	Shao and Granyrd [158]	Round, H	6.0	R-134a	0.189 0.192	183 269
Chitti and Anand [39]	Round, H	8.0	R-22	0.270 0.354	149 438	Cavallini et al. [35]	Round, H	8.0	R-134a, R-419A, R-236ea, R-125, R-32, R-22	0.098 0.553	65 750
Berrada et al. [25]	Round, H	8.92	R-134a, R-22	0.277 0.331	114 308	Altman et al. [7]	Round, H	8.7	R-22	0.289	301 861
Jassim et al. [80]	Round, H	8.9	R-134a	0.163	100 300	Del Col et al. [43]	Round, H	0.96	R-1234yf	0.300	200 1000
Bae et al. [17, 18]	Round, H	12.52	R-12, R-22	0.195 0.0.323	210 634	Jung et al. [83, 84]	Round, H	8.0 8.82	R-142b, R-32, R-125, R-123, R-410A, R-12	0.042 0.553	100 300
Powell [132]	Round, H	12.8	R-11	0.035	258	Tang et al. [163]	Round, H	8.8	R-134a, R-410A, R-22	0.249 0.492	260 820
Son and Lee [161]	Round, H	1.72 5.35	R-134a, R-22, R-410A	0.249 0.482	200 400	Lee et al. [101]	Round, H	10.92	Isobutane, R-22, propylene, propane	0.146 0.361	150
Lee and Son [103]	Round, H	5.8 10.07	Propane, isobutane, R-134a, R-22	0.146 0.321	36 210	Lambrecht et al. [100]	Round, H	8.1	R-22	0.306	300 800
Dalkilic and Agra [41]	Round, H	4.0	Isobutane	0.127	57 92	Eckels and Tesene [59]	Round, H	8.0	R-507A, R-502	0.412 0.502	251 599

(*continued on next page*)

Table 1 (*continued*)

Source	Geometry	$D_{hyd}(D_{HP})$mm	Fluid	p_r	GKg. $m^{-2}s^{-1}$	Source	Geometry	$D_{hyd}(D_{HP})$mm	Fluid	p_r	GKg. $m^{-2}s^{-1}$
Jiang and Garimella [81]	Round, H	9.4	R-404A	0.798 0.896	200 500	Iqbal and Bansal [76]	Round, H	6.52	CO_2	0.309 0.470	50 200
Infante-Ferreira et al. [77]	Round, H	8.0	R-404A	0.485	250 600	Kondou and Hrnjak [95]	Round, H	6.1	CO_2	0.810 0.946	100 200
Hossain et al. [73]	Round, H	4.35	R-32, R-1234ze	0.21 0.427	191 375	Zilly et al. [188]	Round, H	6.1	R-22, CO_2	0.049 0.309	200 400
Akers et al. [3]	Round, H	15.7	R-12, propane	0.657	13 431	Afroz et al. [1]	Round, H	4.35	DME	0.127	200 500
Nan and Infante-Ferreira [128]	Round, H	8.8	Propane	0.285	150 250	Li et al. [106]	Round, H	9.4	R-134a	0.249	100 400
Park et al. [131]	Round, H	8.8	Propylene, isobutane, propane, R-22	0.146 0.361	100 300	Varma (1977)	Round, H	49.0	Water	0.0023	12.6

Note: D_{HP} is listed only if it is different from D_{HYD}.

The correlations that do not involve flow pattern are now discussed. Among them are those of Moser et al. [125], Cavallini et al. [37], and Shah [143,144]. Each of them was based on data from many sources. Most of the data were for macro channels. The data analyzed by Shah included both horizontal and vertical tubes while the other two were verified only with horizontal tube data. The correlations of Ananiev et al. [9] and Akers et al. [3] were based on their own data only but have been compared to other data by many authors.

Many correlations have been proposed exclusively for minichannels. Among them, those verified with most data are those of Kim and Mudawar [93] and Shah [147]. The former is flow pattern based but formulas for predicting flow patterns are included in it.

A few correlations have been published which are intended to be applicable to both mini and macro channels. Among them, those that have been verified with wide-ranging databases are Shah [148,154], Hosseini et al. [190], and Moradkhani et al. [191].

2.3.4. The shah correlations

As the new correlation developed during the present research modifies and incorporates the earlier Shah correlations, they are described here.

Shah [141]. Shah [141] developed the following correlation:

$$h_{TP} = h_{LS}\left(1 + 3.8/Z^{0.95}\right) \quad (1)$$

This correlation is widely used but the author had recommended it only for moderate pressures and higher flow rates.

Shah [143,144]. In order to extend applicability to higher pressures and low flow rates, Shah [143] gave a new correlation. It uses the following two equations.

$$h_I = h_{LS}\left(1 + \frac{3.8}{Z^{0.95}}\right)\left(\frac{\mu_L}{14\mu_G}\right)^{(0.0058+0.557p_r)} \quad (2)$$

$$h_{Nu} = 1.32 Re_{LS}^{-1/3}\left[\frac{\rho_L(\rho_L-\rho_G)gk_L^{\,3}}{\mu_L^{\,2}}\right]^{1/3} \quad (3)$$

Note that Eq. (2) approximates to Eq. (1) when reduced pressure p_r is low. Eq. (3) is the Nusselt equation for condensation in a vertical tube, multiplied by 1.2 as recommended by McAdams [116].

There are three regimes of heat transfer.

In Regime I,

$$h_{TP} = h_I \quad (4)$$

In Regime II,

$$h_{TP} = h_I + h_{Nu} \quad (5)$$

In Regime III:

$$h_{TP} = h_{Nu} \quad (6)$$

h_{LS} in Eqs. (1) and (2) is the heat transfer coefficient of the liquid phase flowing alone in the tube. It is calculated by the following equation:

$$h_{LS} = 0.023 Re_{LS}^{0.8} Pr_L^{0.4} k_L/D \quad (7)$$

Z is the correlating parameter introduced by Shah [141] defined as:

$$Z = (1/x - 1)^{0.8} p_r^{\,0.4} \quad (8)$$

The boundaries of these heat transfer regimes are determined as follows.

Horizontal Tubes:

Regime I occurs when:

$$J_g \geq 0.98(Z + 0.263)^{-0.62} \quad (9)$$

Regime III occurs when:

$$J_g \leq 0.95\left(1.254 + 2.27Z^{1.249}\right)^{-1} \quad (10)$$

If neither of the above conditions is satisfied, it is Regime II.

J_g is the dimensionless vapor velocity defined as:

$$J_g = \frac{xG}{\left(gD\rho_G(\rho_L-\rho_G)\right)^{0.5}} \quad (11)$$

Eq. (11) for the boundary of Regime III was given in Shah [144].

Vertical Downflow:

Regime I occurs when

$$J_g \geq \frac{1}{2.4Z + 0.73} \quad (12)$$

Regime III occurs when:

$$J_g \leq 0.89 - 0.93exp\left(-0.087Z^{-1.17}\right) \quad (13)$$

If the Regime is not determined to be I or III by Eqs. (12) and (13), it is Regime II.

In Shah [146] it was shown that in horizontal tubes, Regime I corresponds to annular flow, Regime II to intermittent and mist flow, and Regime III to stratified flow. The flow patterns were determined by the correlation of El Hajal et al. [60].

Table 2
Range of new data analyzed and deviations of the present and Shah [154] correlations.

Source	Geometry (aspect ratio)#	D_{hyd} (D_{HP})mm	Fluid(Glide, K)**	p_r	GKg. $m^{-2}s^{-1}$	x	Re_{LT}	We_{GT}	Fr_{LT}	N	Deviation, %Mean AbsoluteAverage Shah [154]	Present
Tang et al. [165]*	Round tube, H	6.0	R-410A (0.1)	0.4917	104 476	0.2 0.9	6515 29627	194 4067	0.19 4.0	12	16.3 11.8	10.9 0.5
Ding and Jia [53]	Rectang. channel,H (2.0)	0.67 (1.0)	R-410A (0.1)	0.4457	200 900	0.27 0.83	1962 8821	77 1583	6 123	16	21.6 -20.4	21.6 -20.4
Caruso et al. [32]*	Round tube, H	22.0	Water	0.0046	1.2 5.5	0.0 1.0	96 413	1 19	7.7E-6 1.5E-4	25	14.2 11.2	14.5 11.5
Wu et al. [180]*	Round tube, H	3.8	R-410A (0.1)	0.5809	191 604	0.1 0.8	8359 26451	449 4554	1.1 11.3	12	11.0 2.8	8.6 -6.1
Ren et al. [192]*	Round tube, H	16.0	Water	0.0135	55	0.0 1.0	4256	566	0.022	1	17.0 -17.0	17.0 -17.0
Pusey et al. [133]	Round tube, H	17.0	Water	0.0046	3.4	0.26 0.93	207	6	7.7E-5	3	65.8 65.8	65.6 65.8
	Round tube, VD	17.0	Water	0.0046	3.4	0.26 0.93	207	6	7.7E-5	3	19.4 10.3	19.4 10.3
Kang et al. [86]*	Round tube, H	47.0	Water	0.0272 0.0674	13 27	0.0 1.0	3653 7490	27 134	4.7E-4 2.0E-3	9	21.7 5.2	21.7 5.2
Shen et al. [157]	Round tube, H	18.0	Water	0.0006 0.0014	3.0 7.9	0.31 0.87	99 352	29 200	5.2E-5 3.7E-4	11	19.8 19.8	19.8 19.8
Oh [130]*	Round tube, VD	26.6	Water	0.0087 0.0168	2.9 7.5	0.02 1.0	329 1028	4 15	3.6E-5 2.5E-4	7	19.1 -19.1	19.1 -19.1
Garimella et al. [67]	Round tube, H	7.75	R-245fa	0.0332 0.0803	100 600	0.10 0.86	1798 20597	285 10256	0.07 3,3	86	18.2 8.5	18.2 8.5
			Pentane	0.0402 0.0636	150 600	0.09 0.93	6287 28359	3358 39636	0.82 13.9	64	27.8 27.8	27.8 27.8
		14.4	Pentane	0.0402 0.0954	100 450	0.09 0.87	7787 44398	2773 32273	0.2 4.4	100	5.3 -0.2	5.3 -0.2
Macdonald and Garimella [113]	Round tube, H	7.75	Propane	0.2529 0.9491	150 450	0.10 0.90	12590 53018	1158 10287	1.3 14.5	56	37.5 37.4	37.5 37.4
		14.4		0.2529 0.9491	150 450	0.07 0.92	23458 193504	2158 15E4	0.68 15.9	151	10.2 6.0	10.2 6.0
Toninelli et al. [166]	Square tube, H	1.23	R-134Aa	0.2494	65	0.14 0.56	494	17	0.27	9	26.9 -26.9	26.9 -26.9
			R-1234ze	0.21	100 400	0.08 0.90	735 2942	44 657	0.67 10.7	156	16.7 -16.7	16.7 -16.7
	Round tube, H	0.96	R-134a	0.2494	65 200	0.11 0.94	386 1127	31 1126	0.34 3.2	31	21.0 17.7	21.0 17.7
Mendez et al. [118]	Round tube, H	4.8	R-134a	0.1889 0.2176	200 300	0.02 0.93	5232 8356	694 1478	0.6 1.4	61	31.4 -31.4	31.4 -31.4
Zheng et al. [185]*	Round tube, H	11.5	R-410A	0.5542	49 227	0.2 0.8	6315 29340	87 1897	0.024 0.51	7	12.9 -5.6	7.6 -0.3
Wang et al. [173]*	Round tube, H	8.7	R-134a	0.3292	53 124	0.3 0.9	3025 7666	76 411	0.026 0.15	14	28.3 -28.3	25.5 -25.5
Wang et al. [174]	Round tube, H	4.0	R-1234yf	0.3000	100 400	0.12 0.92	3101 12404	157 2518	0.24 3.8	20	23.3 -23.3	31.4 -31.4
			R-32	0.4271	100 400	0.10 0.91	4203 16812	125 1945	0.32 5.1	21	29.3 -29.3	34.2 -34.2
Lee et al. [104]	Round tube, H	5.2	R-455A (7.6)	0.3677	80 400	0.19 0.81	3510 18366	129 3209	0.12 3.2	16	13.1 13.8	8.2 5.2
			R-454C (3.9)	0.3705	60 400	0.20 0.80	3602 18281	135 3330	0.13 3.2	15	17.9 17.6	10.5 8.6
			R-449A (4.8)	0.3982	80 400	0.20 0.81	3517 17726	110 2583	0.12 3.0	15	10.4 7.3	7.6 -1.3
			R-448A (4.9)	0.4000	80 400	0.20 0.80	3580 18010	106 2452	0.12 3.0	15	19.7 8.5	6.1 0.6
			R-404A (0.3)	0.5463	80 400	0.19 0.81	4369 21826	125 3057	0.14 3.6	13	11.3 8.4	11.9 0.1
Allymehr et al. [5]	Round tube, H	4.1	Propylene	0.2855	200 400	0.17 0.85	9364 18727	1056 4224	4.4 17.5	17	27.7 27.7	10.3 10.3
			Isobutane	0.1275	200 400	0.14 0.89	6011 9017	1541 3466	3.4 17.7	18	21.7 21.7	11.6 11.6
			Propane	0.2855	200 400	0.17 0.85	9364 18727	1056 4224	4.4 17.5	17	27.7 27.7	10.3 10.3

(*continued on next page*)

Table 2 (*continued*)

Source	Geometry (aspect ratio)#	D_{hyd} (D_{HP})mm	Fluid(Glide, K)**	p_r	GKg. $m^{-2}s^{-1}$	x	Re_{LT}	We_{GT}	Fr_{LT}	N	Deviation, %Mean AbsoluteAverage	
											Shah [154]	Present
Sung-Hoon et al. [162]	Round tube, H	5.3	R-134a	0.3234	200	0.11	7462	653	0.63	8	28.1	36.0
						0.82					-28.1	36.0
			R-1234yf	0.3000	100	0.10	4109	208	0.18	68	21.5	22.1
				0.3837	400	0.88	18628	3361	3.1		-6.7	-17.4
		3.7	R-134a	0.2494	100	0.13	2287	121	0.21	8	47.5	51.9
						0.89					-47.5	-51.9
			R-1234yf	0.3399	100	0.08	3052	145	0.27	62	34.0	40.9
				0.3837	400	0.91	13004	2346	4.4		-33.2	-40.9
Baik et al. [21]	Round tube, H	10.7	CO_2	0.7738	500	0.19	80569	11159	4.0	40	30.4	30.4
				0.8692	700	0.86	130609	37033	9.2		30.4	30.4
Qi et al. [134]	Round tube, H	1.0	N_2	0.3071	65	0.17	985	31	1.0	45	18.7	18.7
					262	0.92	3941	489	16.2		-13.0	-13.0
		2.0	N_2	0.3071	13	0.22	394	2	0.02	29	22.8	27.7
					79	0.90	2365	88	0.72		22.8	27.7
Qi et al. [135]	Round tube, VD	1.0	N_2	0.2340	52	0.20	805	19	0.65	82	22.4	10.4
				0.3814	314	0.95	4187	752	213		-16.6	-10.4
		2.0	N_2	0.321	33	0.20	1005	15	0.13	32	41.7	11.8
					79	0.96	2415	88	0.73		41.7	-11.8
Hirose et al. [72]	Round tube, H	3.48	R-152a	0.1750	100	0.19	2391	169	0.38	40	14.4	9.3
					400	0.94	9564	2701	6.1		10.7	3.5
			R-410A	0.4347	100	0.13	3365	100	0.29	31	19.1	12.9
					400	0.98	13456	1617	4.6		14.0	4.1
			R-32	0.3773	100	0.22	3438	105	0.35	39	22.4	16.0
					400	0.97	13754	1679	5.6		10.3	1.3
Bashar et al. [20]	Round tube, H	2.14	R-134a	0.1402	50	0.02	515	22	0.079	84	20.5	20.5
				0.1889	300	0.96	3499	696	3.0		-15.4	-15.4
Mazumdar et al. [115]	Round tube, H	4.33	R-407C (5.1)	0.3316	307	0.04	9801	1225	1.9	15	21.2	27.6
					403	0.97	12828	1946	3.2		-21.2	-27.6
			R-1234ze	0.2100	307	0.10	7946	1446	1.8	12	30.8	37.4
					403	0.95	10430	2492	3.1		-30.8	-37.4
			R-32	0.4271	307	0.01	13968	1240	2.8	16	21.4	24.9
					403	0.97	18336	2137	4.8		-19.6	-24.9
Keniar and Garimella [89]	Square tube, H	0.98	R-1234ze	0.1584	100	0.22	520	39	0.79	27	30.2	30.2
					300	0.89	2082	627	12.7		-30.2	-30.2
			R-134a	0.1889	100	0.24	534	35	0.74	26	30.7	30.7
					400	0.87	2127	567	11.8		-30.7	-30.7
	Round tube, H	1.55	R-1234ze	0.1584	50	0.19	412	15	0.12	31	20.8	20.8
					200	0.87	1646	248	2.0		-13.9	-13.9
			R-245fa	0.0484	50	0.19	206	29	0.09	32	18.0	18.0
					200	0.84	619	471	1.5		-17.8	-17.8
			R-134a	0.1889	50	0.11	442	14	0.12	47	23.3	23.3
				0.2494	150	0.87	1437	114	1.1		-22.4	-22.4
Kim et al. [92]	Rectang.Multi, H (0.46)	0.8	R-455A (7.6)	0.3677	380	0.26	2565	447	18	8	16.5	16.5
					760	0.69	5348	1774	75		10.5	10.5
			R-454C (3.9)	0.3705	380	0.26	2632	468	19	8	19.0	19.0
					760	0.69	5342	1849	75		15.9	15.9
			R-449A	0.3982	380	0.25	2570	383	17	8	16.5	16.5
					760	0.67	5171	1427	69		13.9	13.9
			R-448A	0.4000	380	0.26	2616	367	17	9	21.0	21.0
					760	0.87	5255	1365	70		19.3	19.3
			R-404A (0.3)	0.5463	380	0.32	3193	433	21	8	26.6	26.6
					760	0.71	6381	1698	84		26.6	26.6
Jacob et al. [78]	Round tube, H	4.7	R-134a	0.2846	299	0.01	6197	593	0.68	68	13.8	8.3
				0.3661	600	0.97	2134	5159	6.7		12.4	2.1
			R-450A	0.2588	100	0.02	3141	135	0.18	103	14.8	7.4
				0.3328	550	0.95	19750	3841	6.0		14.1	0.4
Azzolin et al. [15]	Round tube, H	0.96	R-455A (9.5)	0.3209	200	0.14	1506	144	4	49	7.2	7.2
					800	0.81	6381	2339	67		6.8	6.8
			R-452B (3.8)	0.3916	200	0.16	1841	134	4.6	41	15,6	15.6
					800	0.87	7403	2126	74		15.5	15.5
		8.0	R-455A (9.5)	0.3209	100	0.13	6276		0.14	60	8.8	8.8
					600	0.90	39922	10976	4.5		-6.3	-6.3
			R-452B (3.8)	0.3916	100	0.17	7671	279	0.14	51	12.4	12.4
					600	0.94	46325	10031	5		-1.2	-1.2
Azzolin et al. [16]	Round tube, H	3.4	R-134a	0.2494	50	0.14	1051	28	0.06	74	9.4	13.6
					200	0.91	4204	445	0.91		-6.1	-12.9
	Round tube, VD	3.4	R-134a	0.2494	50	0.26	1051	28	0.06	106	27.3	16.8
					200	0.93	4204	445	0.91		16.2	10.9

(continued on next page)

Table 2 (*continued*)

Source	Geometry (aspect ratio)#	D_{hyd} (D_{HP})mm	Fluid(Glide, K)**	p_r	GKg. $m^{-2}s^{-1}$	x	Re_{LT}	We_{GT}	Fr_{LT}	N	Deviation, %Mean AbsoluteAverage	
											Shah [154]	Present
Meyer and Ewim [120]_	Round tube, H	8.34	R-134a	0.2494	50 200	0.09 0.90	2578 10312	68 1091	0.023 0.37	91	14.1 -2.9	10.5 0.8
Ewim et al. [61]	Round tube, H	8.34	R-134a	0.2494	50 100	0.25 0.75	2590 5181	68 274	0.023 0.092	36	24.9 -15.4	15.6 -4.4
	Round tube, VD	8.34	R-134a	0.2494	50 100	0.25 0.75	2590 5181	68 274	0.023 0.092	36	24.0 11.2	24.0 11.2
Moreira et al. [124]	Round tube, H	9.43	R-134a	0.2176	100 250	0.15 0.95	5472 13680	323 2016	0.08 0.49	30	16.2 8.5	16.2 8.5
			Propylene	0.3215	50 250	0.08 0.95	5401 27004	131 3274	0.11 2.8	40	15.4 8.2	15,4 8.2
			Iobutane	0.1275	50 250	0.04 0.93	3456 17282	221 5536	0.09 2.3	32	16.2 8.0	16.2 8.0
			Propane	0.2855	50 250	0.04 0.90	5384 26920	152 3795	0.12 3.0	39	12.0 -3.7	12.0 -3.7
Diani et al. [52]	Round tube, H	3.4	R-513A	0.2106 0.2757	100 1000	0.19 0.93	2110 23889	131 12180	0.24 26	102	28.0 27.4	17.3 16.0
Li et al. [109]*	Annulus, H OD/ID 17/12.7 mm	4.3 (10.5)	R-410A (0.1)	0.4347 0.5542	75 225	0.2 0.8	8830 26482	76 693	0.15 1.3	13	10.3 5.1	10.8 -4.5
Borchmann [28]*	Annulus,H, OD /ID 38/ 31.2	6.8 (15.0)	R-11	0.0373	29 286	0.55 1.0	1245 12278	39 3747	0.006 0.59	5	30.3 -30.3	30.3 -30.3
Solanki and Kumar [160]	Round tube, H	8.91	R-134a	0.2176 0.2846	450 650	0.12 0.80	23266 33607	6173 12880	1.7 3.5	19	10.6 -0.6	10.6 -0.6
Kim et al. [91]	Round tube, H	5.6	R-404A (0.3)	0.5463	80 200	0.21 0.80	4705 11753	134 823	0.13 0.83	9	3.5 3.2	4.2 -4.2
Sarmadian et al. [139]	Round tube, H	8.3	Isobutane	0.1454	114 368	0.08 0.8	7294 23546	948 9878	0.56 5.9	33	12.0 9.5	12.0 9.5
Ghim and Lee [69]	Round tube, H	7.7	HFE-7000	0.0785 0.1372	150 500	0.01 0.75	3809 15195	1948	0.17 2.1	52	22.4 20.3	22.4 20.3
Kozistky et al. [97]*	Round tube, VD	40.0	R-22	0.2379	1.0 2.9	0.5	252 750	< 1	1.8E-6 1.5E-5	7	20.7 -20.7	20.7 -20.7
			R-12	0.1654	1.1 4.3	0.5	236 941	< 1	1.8E-6 2.8E-5	5	19.9 -19.9	19.9 -19.9
Kurita et al. [99]*	Round tube, VD	6.6	FC-72	0.0167 0.0895	7.3 29.5	0.5	78 441	8 82	2.9E-4 5.2E-3	12	39.6 38.9	4.1 2.4
All Sources (36)		0.5 22.0		0.0006 0.9491	1.2 1360	0.01 1.0	96 193504	1 37033	7.7E-6 4070	2931	19.5 2.4	17.3 -1.4

* Mean htc data. Inlet and outlet quality is listed, their arithmetic mean used.
** Glide is listed only when > 0.
# Aspect ratio is listed only when it is not 1.

Shah (2016, 2019) correlations. Shah [147] analyzed data for horizontal minichannels and found that heat transfer coefficients at low flow rates were higher than predicted by the Shah [144] correlation. He reasoned that this may be because of surface tension forces becoming stronger than the inertia forces at low flow rates. As Weber number is the ratio of inertia and surface tension forces, the enhancement in heat transfer may be related to it. He found that it occurs when $We_{GT} < 100$. It is defined as:

$$We_{GT} = \frac{G^2 D}{\rho_G \sigma} \tag{14}$$

Regime I became Regime II when $We_{GT} < 100$, thus increasing the predicted heat transfer coefficient.

Shah [147] found that somewhat better accuracy is obtained if Eq. (2) is replaced by the following equation developed by Cavallini et al. [38] for their ΔT- independent regime.

$$h_I = h_{LT}\left[1 + 1.128x^{0.817}\left(\frac{\rho_L}{\rho_G}\right)^{0.3685}\left(\frac{\mu_L}{\mu_G}\right)^{0.2363}\left(1 - \frac{\mu_G}{\mu_L}\right)^{2.144} Pr_L{}^{-0.1}\right] \tag{15}$$

In Shah [148], data for all channel diameters in all orientations was analyzed. Regime III was found to occur only if $We_{GT} > 20$. It was found that Eq. (15) gives lower deviations only for horizontal channels with $D \leq 3$ mm. For vertical downflow in channels of all sizes and horizontal flow in channels of $D > 3$ mm, use of Eq. (2) gave better agreement with data. Data for inclinations other than horizontal and vertical downflow were found to be in satisfactory agreement using the correction factor given in Shah (2015) to take into account the effect of inclination.

Shah [154] collected additional data for horizontal and vertical downflow and compared it to the Shah [148] correlation. The following modifications were made. Shah [144] correlation was to be used if $Re_{LT} < 100$, and for hydrocarbons if $p_r < 0.4$. For conditions other than those, the following modifications were made. Regimes I and III occurred in horizontal tubes only if $Fr_{LT} > 0.012$. For vertical downflow, flow regimes were determined the same way as in Shah [147]. The Shah [154] correlation showed good agreement with data from 88 sources, significantly better than other correlations.

3. The improved shah correlation

3.1. Development

The entire database was compared to the Shah [154] correlation. Examination of the output indicated that the accuracy of the correlation could be improved by making some changes as described below.

3.1.1. Vertical downflow

In the Shah [154] correlation, heat transfer in vertical downflow is higher at $We_{GT} < 100$ in the same way as in horizontal flow. This was based on a few data sets. One of these showed strong effect of Weber number while for others, the deviations were within ± 30% with or without the effect of We_{GT}. Several more data sets for vertical flow were analyzed this time. It was found that for these data sets, most data at $We_{GT} < 100$ were over-predicted by Shah [154] correlation and were in satisfactory agreement with Shah [144] correlation. For some data at low Re_{LT} and We_{GT}, Shah [144] was found to be over-predicting. Investigation showed that Shah [144] was predicting Regime II while the measured heat transfer coefficients were agreeing with the Nusselt equation which is used for Regime III in Shah correlations. This result is in agreement with what will be expected from physical reasoning. In the absence of significant shear by vapor, the liquid film will be expected to remain laminar and heat transfer will be according to the Nusselt model. For all such data points, We_{GT} was less than 100 and hence the vapor velocity was low. Study of available test data showed that when $Re_{LT} < 600$ and $We_{GT} < 100$, Regime is III. Hence the criterion in Shah [144] for occurrence of Regime III, Eq. (12) needs to be modified to include this criterion.

Based on the discussions in the above paragraph, it was decided to use the Shah [144] correlation modified to include the additional criterion for Regime III occurrence, for vertical channels. It greatly reduced the MAD compared to Shah [154].

The reason why low We_{GT} does not enhance heat transfer in vertical channels while it enhances heat transfer in horizontal ones is suggested by the flow patterns in the two orientations. Many visual studies of condensation flows have been made. A good recent study is by Azzolin et al. [15,16] who made observations on the same tube in horizontal and vertical downflow. In vertical flow, annular flow with liquid layer of uniform thickness was seen over the entire range of flow rates from 50 to 200 $kgm^{-2}s^{-1}$ and vapor qualities 0.11 to 0.89. In horizontal flow over the same range, flow patterns varied from stratified to slug to annular, the thickness of the liquid at the bottom being mostly thicker. It appears that surface tension thins out the liquid film when liquid distribution is asymmetrical as in horizontal flow but does not have effect when liquid distribution is uniform as in vertical flow.

3.1.2. Horizontal flow

Effect of froude number. In Shah [154] for horizontal flow, Regimes I and III occur only if $Fr_{LT} > 0.012$, otherwise Regime II occurs in which heat transfer coefficients are higher. Analysis of all data including the new data, it was found that deviations were minimized if the transition was changed to $Fr_{LT} < 0.026$. Thus, the transition point has moved closer to the start of stratification at $Fr_{LT} < 0.04$ in the Shah [140] correlation for boiling in tubes.

Hydrocarbons. In Shah [154], Weber number affects heat transfer to hydrocarbons only when $p_r > 0.4$. The only data for p_r were a few for a vertical channel from one source. As there are no data for horizontal tubes for $p_r > 0.4$, it was decided to remove this limit. In the improved correlation, heat transfer coefficients for hydrocarbons are always calculated with the Shah [144] correlation, irrespective of the value of p_r, Fr_{LT}, and We_{GT}.

Transition channel diameter. In Shah [154], h_I is calculated with Eq. (2) when $D_{HYD} > 3$ mm and by Eq. (15) when $D_{HYD} \le 3$ mm. Analysis of the present enlarged database showed that deviations are minimized if the transition is at 6 mm diameter. Thus, except where Shah [144] correlation is used, h_I is calculated with Eq. (2) when $D_{HYD} > 6$ mm and by Eq. (15) when $D_{HYD} \le 6$ mm. Where Shah [144] is used such as for hydrocarbons, h_I is always calculated with Eq. (2) irrespective of the diameter size.

3.2. The final improved correlation

Based on the developments described above**,** the improved correlation is as below.

Use the modified Shah [144] correlation for any of the following conditions:

1 Vertical downflow.
2 Hydrocarbons in all orientations.
3 $Re_{LT} < 100$, any orientation.

The modified Shah [144] correlation differs from the Shah [144] correlation given in Section 2 only in the criteria for Regime III in vertical flow, as stated below.

For vertical downflow, Regime III occurs if Eq. (13) is satisfied or if $Re_{LT} < 600$ and $We_{GT} < 100$.

For vertical downflow, Eq. (2) to be used to calculate h_I. Use D_{HP} in calculating Re_{LT} and h_I. Definitions of equivalent diameters are:

$$D_{HP} = \frac{4\ x\ Flow\ area}{Perimeter\ with\ heat\ transfer} \tag{16}$$

$$D_{HYD} = \frac{4\ x\ Flow\ area}{Wetted\ Perimeter} \tag{17}$$

For horizontal channels:

Regime I occurs if $We_{GT} > 100$ and $Fr_{LT} > 0.026$ and:

$$J_g \ge 0.98(Z + 0.263)^{-0.62} \tag{18}$$

Regime III occurs if $Fr_L > 0.026$ and:

$$J_g \le 0.95(1.254 + 2.27Z^{1.249})^{-1} \tag{19}$$

If it is not Regime I or III, it is Regime II.

In Regime I,

$$h_{TP} = h_I \tag{20}$$

In Regime II,

$$h_{TP} = h_I + h_{Nu} \tag{21}$$

In Regime III:

$$h_{TP} = h_{Nu} \tag{22}$$

For $D_{HYD} \le 6$ mm, calculate h_I with Eq. (15).

For $D_{HYD} > 6$ mm, calculate h_I with Eq. (2).

Use D_{HP} in calculating Re_{LT} and h_I. Use D_{HYD} in calculating We_{GT} and $Fr_{LT.}$

4. Evaluation of correlations

The improved correlation as well as a number of other correlations were compared to the database that included the data collected during the present project as well as the data analyzed in Shah [154] except those of Wilson et al. [179] for channels formed by flattening of round tubes. The reason for this exclusion is discussed in Section 5.4.2.

4.1. Data collection and selection

Efforts were made to collect a wide range of data especially for new fluids and conditions not included in the database used in Shah [154]. Data for refrigerants containing oil were not considered as presence of oil affects heat transfer. Data for zeotropic mixtures with significant glide were not considered earlier but have been included now. The data collected during the present research are listed in Table 2. Those analyzed in Shah [154] are listed in Table 1. The complete range of data in the current database which includes both newly collected and previously analyzed data is listed in Table 3. A significant addition to the previous database is eight new fluids that include nitrogen; there had been no cryogenic fluid in the earlier database. Another important addition is the data for annuli; there were none before.

The data of Baik and Yun [21] for carbon dioxide at p_r of 0.98 were not included. The reason is that so close to the critical point, fluid properties are greatly affected by small changes in temperature. Under such conditions, it will be more appropriate to use properties at film temperature but it was not possible to do so as test data did not provide wall temperatures.

The data of Komanditivirya et al. [94] and Volrath et al. [171] for ammonia were not included for reasons discussed in Section 5.7.

4.2. Prediction methods evaluated

Only the methods which have been shown to agree with data for many fluids from many sources by the authors themselves or by others were considered. The ones that meet this criterion have been mentioned in Section 2. Among them, some require that ΔT or heat flux be known. These are those of Dobson and Chato [55], Thome et al. (2003), and Cavallini et al. [37]. These could not be evaluated as heat flux or ΔT is not given in most publications. The predictive methods evaluated are those of Traviss et al. [167], Ananiev et al. [9], Kim and Mudawar [93], Hosseini et al. [190], Moradkhani et al. [191], Dorao and Fernandino [57], Moser et al. [125], Akers et al. [3], Shah [141,144,154]. The Shah [147,148] correlations were also evaluated but the results are not given or discussed as they are very close to those of Shah [154] correlation. The results for Shah [141] are not included in the tables as this was intended only for low pressures and high flow rates. Its performance and range of applicability is discussed in Section 5.10.

4.3. Calculation methodology

In analyzing the data of Son and Lee [161], single phase heat transfer was calculated by the following equation instead of Eq. (7):

$$h_{LS} = 0.034\mathrm{Re}_{LS}^{0.8}\,\mathrm{Pr}_L^{0.3}\,k_L/D \tag{23}$$

The reason is that the single-phase heat transfer measurements of these authors were much higher than Eq. (7) and instead agreed with this equation.

The predicted heat transfer coefficients by all correlation for zeotropic mixtures were corrected by the method of Bell and Ghaly [24] as follows.

$$\frac{1}{h_{mix}} = \frac{1}{h_c} + \frac{Y_G}{h_{GS}} \tag{24}$$

Where,

$$Y_G = xC_{pg}\frac{dT_{glide}}{dT} \tag{25}$$

h_c is the condensing heat transfer coefficient calculated with mixture properties using a correlation for pure fluids. h_{GS} is the superficial heat transfer coefficient of the vapor phase, i. e. assuming vapor phase to be flowing alone in the tube, calculated by the following equation.

$$h_{GS} = 0.023\left(\frac{GxD}{\mu_G}\right)^{0.8} Pr_G^{0.4}\frac{k_G}{D} \tag{26}$$

In calculations with all Shah correlations, D_{HP} was used in calculating single phase heat transfer coefficient and Reynolds number. The same was also done with other correlations except those

Table 3
Range of test data analyzed. Changes from Shah [154] are italicized.

Parameter	Data Range
Fluids	Water, R-11, R-12, R-22, R-32, R-41, R-113, R-123, R-125, R-134a, R-141b, R-142b, R-152a, R-161, R-236ea, R-245fa, R-404A, R-410A, *R-448A*, *R-449A*, *R-450A*, R-502, R-507, *R-513A*, *R-452B*, *R-454C*, *R-455A*, R-1234fa, R-1234yf, R-1234ze(E), DME, butane, propane, carbon dioxide, methane, FC-72, isobutane, propylene, benzene, ethanol, methanol, toluene, Dowtherm 209, HFE-7000, HFE-7100, ethane, pentane, Novec 649, ammonia, *nitrogen* (51 fluids)
Geometry	Round, square, rectangle, semi-circle, triangle, and barrel shaped single & multi channels. All sides cooled or one side insulated. Cooled partly or on all sides. *Annuli.*
Orientation	Horizontal, vertical down
Aspect Ratio, width/height	0.14 to *2.0*
D_{HYD}, mm	0.08 to 49.0
Reduced pressure	*0.0006* to *0.949*
G, kg m^{-2} s^{-1}	1.1 to 1400
x, %	0.01 to 0.99
We_{GT}	0.15 to 79060
Fr_{LT} for horizontal channels	*7.7E-6* to 4070
Glide of mixtures, K	*0.1 to 9.5*
Bond number	0.033 to 2392
Number of data sources	*130* (*110* Horizontal, *16* vertical down, 4 both)
Number of data sets	262 (233 horizontal, 29 vertical down)

Table 4
Effect of orientation, diameter, and Weber number on deviations of various correlations from data.

Orientation	Dia. mm	We_{GT}	N	Deviation, %Mean AbsoluteAverage										
				Shah [144]	Shah [154]	Present	Kim & Mudawar	Ananiev et al.	Dorao & Fer-nandino	Hosseini et al	Moradkhani et al.	Moser et al.	Traviss et al.	Akers et al.
Horizontal	≤ 3	< 100	788	31.8	20.4	20.5	29.7	41.6	43.0	40.2	28.5	32.9	40.8	152.3
				-24.0	-2.2	-2.0	-19.0	-38.0	-40.8	-31.7	-21.1	-5.2	15.2	125.9
	≤ 3	> 100	2033	21.3	18.5	18.5	19.4	19.7	19.8	22.3	20.8	34.1	99.4	105.4
				6.7	-1.9	-1.9	-8.5	-8.2	-7.4	-3.5	-6.7	26.3	95.8	103.8
	≤ 3	All	2821	24.2	19.0	19.1	22.3	25.8	26.3	27.3	22.9	33.3	88.1	116.3
				-1.9	-2.0	-1.9	-11.4	-16.5	-16.7	-11.4	-19.9	17.5	17.8	114.9
	> 3	< 100	255	29.0	27.1	26.1	65.0	56.4	61.5	47.4	38.3	43.8	43.5	36.2
				-9.6	-4.7	6.2	8.6	-56.4	-61.6	5.4	-29.5	-41.6	-10.7	-0.2
	> 3	>100	4412	17.5	17.3	16.6	26.2	23.4	23.3	28.2	17.4	33./7	118.3	26.8
				3.0	3.3	0.7	-21.1	-13.1	-15.4	4.8	-2.4	19.5	113.3	-4.2
	> 3	All	4667	18.2	17.4	17.1	28.7	25.1	25.4	29.2	18.5	34.2	114.3	27.3
				2.3	1.9	1.0	-19.9	-15.3	-18.8	4.9	-3.9	16.3	106.7	-4.0
	All	All	7488	20.2	18.3	17.8	26.3	25.2\-	25.6	29.1	20.2	34.0	104.0	62.5
				5.1	1.1	-0.1	-16.7	15.5	-17.3	-1.1	-6.2	16.9	95.7	43.1
Vertical Downflow	≤ 3	all	272	20.7	26.4	20.7	23.7	28.6	25.4	32.9	19.6	31.3	69.4	128.0
				-5.9	2.2	-5.9	-8.2	-21.8	-19.1	-14.8	2.4	6.6	66.2	128.0
	> 3	all	538	16.7	18.8	15.8	40.2	33.8	38.8	40.5	31.1	33.2	60.1	42.7
				2.8	6.2	1.9	14.1	-1.5	-35.4	15.0	6.4	6.4	39.0	4.6
	All	All	810	18.0	21.4	17.4	34.7	32.1	34.3	37.9	27.2	32.5	63.2	71.3
				-0.1	4.8	-0.1	6.6	-8.3	-29.9	5.0	3.4	6.5	48.1	46.0
Hor. & Vert.	All	< 100	1271	29.7	23.8	21.7	42.4	44.9	47.6	43.6	31.2	35.7	42.9	121.1
				-17.9	1.2	-1.5	-6.3	-42.3	-46.0	-21.0	-21.3	-15.4	10.5	108.9
		> 100	7027	18.5	17.6	17.1	24.3	22.7	22.8	26.9	19.0	33.8	110.8	52.6
				4.0	1.5	0.1	-15.9	-10.0	-13.8	3.0	-2.5	21.8	106.3	31.2
	All	All	8298	20.2	18.6	17.9	26.1	26.1	26.6	29.4	20.9	34.0	97.8	62.6
				0.6	1.4	-0.1	-14.4	-15.0	-18.7	-0.6	-5.2	16.0	88.0	42.5
														43.1

of Kim and Mudawar [93], Dorao and Fernandino [57], Hosseini et al. [190], and Moradkhani et al. [191]. For these correlations, D_{HYD} was used as the diameter in all calculations because that was specified by these authors.

Where the authors reported mean heat transfer coefficient data, they were analyzed using the arithmetic mean quality.

Properties of HFE-7100, and FC-72 were obtained from their manufacturer 3-M Corporation. Properties of Dowtherm 209 were taken from Blangetti and Schlunder [27]. Surface tension of HFE-7000 was taken from Vins et al. [170]. All other properties were obtained from REFPROP 9.1, Lemmon et al. [105]. All properties used were at saturation temperature.

4.4. Results of data analysis

Table 2 lists the deviations of the Shah [154] and the present correlation with the new data collected during the present research. The predictions of all correlation for zeotropic mixtures have been corrected by the Bell and Ghaly [24] method. The deviations listed in it are defined as:

Mean absolute deviation (MAD) is defined as:

$$MAD = \frac{1}{N}\sum_{1}^{N} ABS\left\{\left(h_{predicted} - h_{measured}\right)/h_{measured}\right\} \quad (27)$$

Average deviation (AD) is defined as:

$$AD = \frac{1}{N}\sum_{1}^{N}\left\{\left(\mathrm{h}_{\mathrm{predicted}} - \mathrm{h}_{\mathrm{measured}}\right)/\mathrm{h}_{\mathrm{measured}}\right\} \quad (28)$$

It is seen that the MAD of the present correlation is 17.3% compared to 19.5% for the Shah [154] correlation. In Table 4, the deviations of the various correlations for the entire database are listed. The MAD of the present correlation for all 8298 data points from 130 sources is seen to be 17.9% which is significantly lower than of the other correlations. The Shah [154,144] have MAD of 18.6% and 20.2%, respectively. The next best is Moradkhani et al. [191] with a MAD of 20.9%. MAD of the correlations of other authors range from 26.1% to 97.8%. The highest MAD are of the correlations of Traviss et al. and Akers et al., 97.8% and 62.6 %, respectively.

From the foregoing, it is clear that the new correlation is the most accurate over the entire range of data. The range of applicability of the other correlations can be inferred from the results in Table 4 and is further discussed in Section 5. It is clear from the results in Tables 2 and 4 that the correlations of Moser et al., Traviss et al., and Akers et al. have large deviations with most data and thus are unreliable. These are therefore excluded from further discussions except where specifically mentioned.

5. Discussion

5.1. Effect of orientation

Table 4 lists the deviations of all correlations for different channels sizes, orientations, and Weber numbers.

For all data for horizontal channels, the MAD of the present correlation is 17.8% which is better than 18.3% of the Shah [154] correlation. The MAD of the correlations of other authors varies from 20.2% of the Moradkhani et al. [191] correlation to 104% of the Traviss et al. analytical correlation.

For all data for vertical channels, the MAD of present correlation is 17.4% while that of Shah [154] correlation is 21.4%, a considerable improvement. The MAD of the correlations of other authors ranges from 27.2% to 71.3%. This indicates that for vertical flow, the present correlation is by far the best choice. Among the correlations of other authors, the only one which makes reasonably accurate predictions is that of Moradkhani et al. [191] which has MAD of 27.2%.

Fig. 1 compares the data of Qi et al. [135] for nitrogen in a vertical tube with several correlations. The predictions of the present

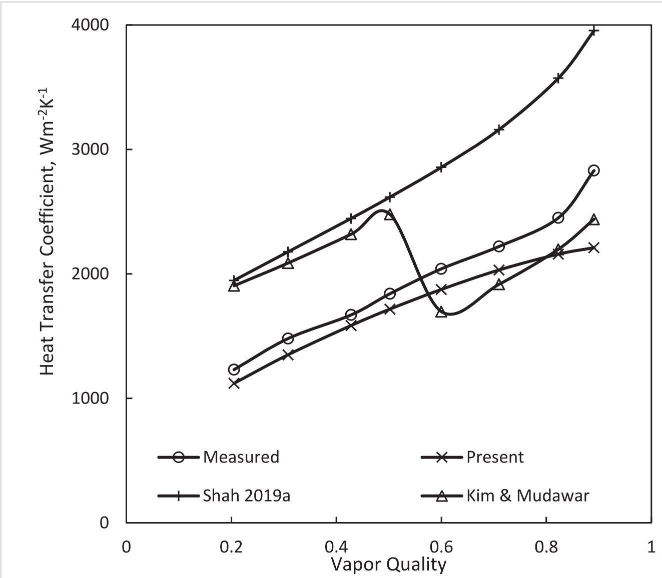

Fig. 1. Comparison of the data of Qi et al. [135] for nitrogen in vertical downflow with the present and other correlations. D = 2 mm, T_{SAT} = -167.9 °C, G = 52.4 kgm^{-2}s^{-1}, We_{GT} = 39.

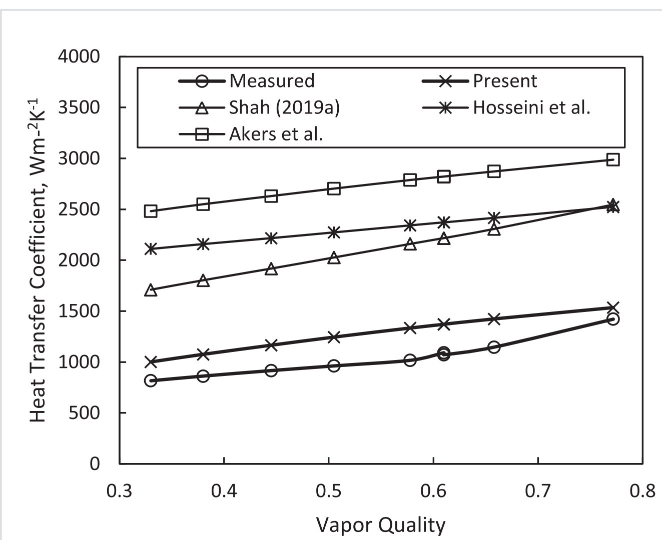

Fig. 2. Comparison of the present and other correlations with the data of Azzolin et al. [16] for R-134a in a vertical tube 3.4 mm diameter. T_{SAT} = 40 °C, G =75 kgm^{-2}K^{-1}, We_{Gt} = 63. Note the improvement compared to Shah [154].

correlation are close to the measured heat transfer coefficients while Shah [154] predicts much higher.

Fig. 2 shows the comparison of the data of Azzolin et al. [16] in a vertical tube with several correlations. The present correlation shows close agreement with data while Shah [154] predicts much higher. Other correlations also show large deviations. This improvement is due to the change in the criterion for occurrence of Regime III as discussed in Section 3.1.1.

5.2. Effect of weber number

As was discussed in Section 3.1.1, present research led to the conclusion that in vertical downflow, We_{GT} has no effect to heat transfer except when $We_{GT} < 100$ together with $Re_{LT} < 600$. Heat

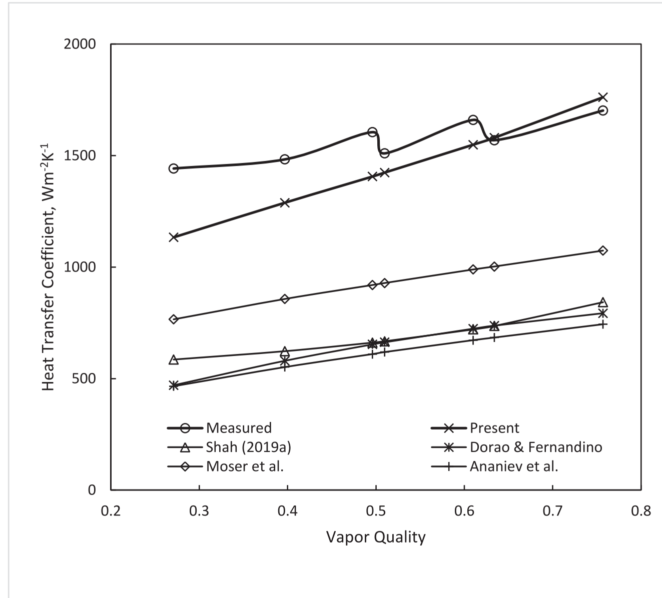

Fig. 3. Comparison of the data of Meyer and Ewim [120] with pthe present and other correlations. R-134a, D = 8.34 mm, T_{SAT} = 40 °C, G = 50 kgm^{-2}s^{-1}, Fr_{LT} = 0.023, We_{GT} = 68. Note the improvement of the present correlation over Shah [154] resulting from the change in transition Fr_{LT}.

transfer coefficient is then lower than prediction of Shah [154] correlation. This indicates change in heat transfer regime from II to III.

Low We_{GT} has a profound effect on heat transfer during horizontal flow as seen in Table 4. For $D_{HYD} \leq 3$ mm, it is seen that all correlations other than the present and Shah [154] greatly underpredict the data when $We_{GT} < 100$, their average deviation ranging from -19 to -40.8% while their MAD ranges from 28.5% to 43%. When $We_{GT} > 100$, the deviations of all those correlations greatly improve. For example, the MAD of the Dorao and Fernadino correlation decreases from 43% to 19.8% and that of Hosseini et al. from 40.2 to 22.3%. The correlation of Kim and Mudawar was developed specifically for minichannels but the results for it are similar.

Similar results are also with data for $D_{HYD} > 3$ mm. The AD of Dorao and Fernandino correlation is -61.6% when $We_{GT} < 100$ and -15.45 when $We_{GT} > 100$; the corresponding MAD are 61.6% and 23.3%. The MAD of Kim and Mudawar is 65% and 26.2%, respectively for $We_{GT} < 100$ and $We_{GT} > 100$. Fig. 3 shows data for a tube of 8.3 mm diameter with $We_{GT} = 69$. The present correlation gives good agreement with data due to the effect of low Weber number while other correlations greatly underpredict.

5.3. Boundary between mini and macro channels

Most researchers consider the boundary of minichannels to start when surface tension begins to affect heat transfer and therefore correlations based on macro (conventional) channel data begin to fail. It is evident from the discussions in Section 5.2 that the commonly used criterion of $D \leq 3$ mm does not correspond to the start of the effect of surface tension. For horizontal channels, this boundary is at $We_{GT} < 100$. For vertical channels, the present data analysis indicates that the macrochannel correlation of Shah [144] gives satisfactory agreement with data for $D < 3$ mm even when $We_{GT} < 100$. The smallest diameter in the data analyzed for vertical channels when $We_{GT} < 100$ is 1 mm.

Table 5
Deviations of the more accurate correlations for different shapes and types of channels.

Shape	Sigle or Multi	N	Deviation, %Mean AbsoluteAverage Shah [144]	Shah (2019)	Present	Kim & Mudawar	Ananiev et al.	Dorao & Fernandino	Hosseini et al	Moradkhani et al.
Round	Both	6967	19.1	18.3	17.3	27.8	25.9	26.4	29.1	20.6
			1.7	2.2	0.5	-14.9	-14.2	-18.9	2.3	-4.2
	Single	6819	19.0	18.3	17.3	28.1	26.0	26.6	29.2	20.6
			1.5	2.1	0.3	-15.2	-14.3	-19.2	2.4	-4.3
	Multi	148	21.0	17.2	17.1	12.9	17.3	17.7	24.0	17.4
			7.8	9.6	10.3	-1.3	-1.3	-5.0	0.9	-1.5
Non-circular	Both	1331	26.3	20.3	20.3	23.4	27.3	27.6	31.2	22.5
			-4.7	-2.3	-3.7	-12.0	-18.7	-17.9	16.3	-10.0
	Single	475	22.3	17.8	18.3	23.5	28.3	28.5	28.1	19.2
			-10.5	-7.9	-11.0	-19.0	-25.0	-24.1	-19.2	-12.2
	Multi	856	28.5	21.2	21.4	23.3	26.7	27.1	32.8	24.4
			-1.4	0.2	0.4	-8.1	-15.1	-14.3	-14.2	-9.6

5.4. Impact of channel shape

5.4.1. Channels with sharp corners

Wang and Rose [175,176] performed mechanistic analyzes assuming laminar flow of condensate. They concluded that heat transfer in square and rectangular channels is higher than in round tubes because of the thinning of condensate film caused by surface tension pushing liquid into the corners. Table 5 shows the results of the present data analysis for circular and non-circular channels. The non-circular channels' shapes included square, rectangular, triangular, etc. all of them have sharp corners. The average deviation of the present correlation with data for round channels is 0.5% while that for non-circular channels is -3.7%. The deviations of the Kim and Mudawar correlation are -14.9% and -12% for round and non-circular channels, respectively. Deviations of other correlations are also similar. These results do not show that channels with sharp corners have higher heat transfer than the round channels which have no sharp corners. The theory of Wang and Rose had assumed laminar liquid film. Many experimental and theoretical studies have shown that vapor shear caused condensate film to become turbulent at very low Reynolds numbers. For example, Carpenter and Colburn [31] found during their tests on condensation in a tube that the liquid film turned turbulent at a liquid Reynold number of 240. Rohsenow et al. [138] analyzed condensation on a vertical plate. The transition liquid Reynolds number was found to decrease to as low as 50 with increasing vapor shear. Kim and Mudawar [90] analyzed condensation in a rectangular channel. Transition to turbulence was found at liquid Reynolds number of 25. Shah [152,153] analyzed data for heat transfer to gas-liquid flow in tubes. Transition to turbulent film was found to be at Re_{LS} of 170-175. It is thus clear that liquid layer is laminar only over a very short length of channel and hence the theory of Wang and Rose is inapplicable over most of the tube length.

Fig. 4 compares the present and other correlations with data for a rectangular channel. Good agreement of the present correlation with data is seen.

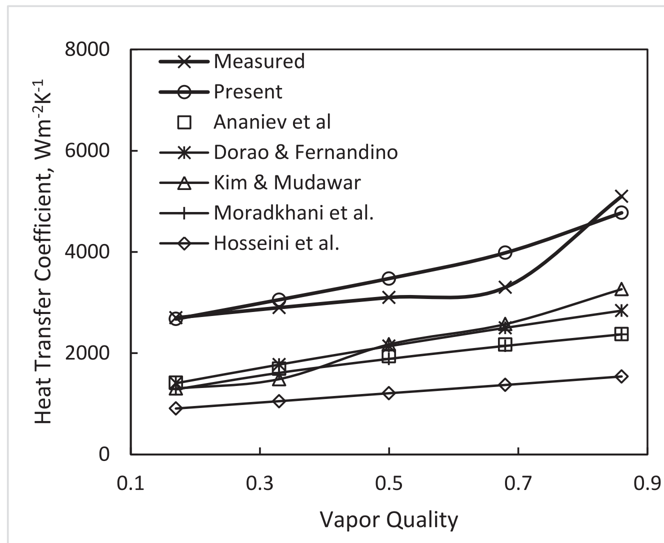

Fig. 4. Comparison of present and other correlations with the data of Jige et al. [82] for R-32 in a horizontal multichannel with rectangular channels of aspect ratio 0.69. $D_{HYD} = D_{HP} = 0.85$ mm. $T_{SAT} = 60$ °C, G = 100 kgm^{-2}s^{-1}.

5.4.2. Channel aspect ratio

Fig. 5 shows the comparison of the present correlation with data from non-circular channels other than those for flattened tubes. The three data points with MAD of over 70% are from Garimella et al. [66]. These are very high compared to all correlations and hence are very unusual. Their deviation is the same at all three aspect ratios. The other data are for aspect ratios 0.14 to 2. The deviations of almost all are low and no effect of aspect ratio is apparent.

Note that the data of Wilson et al. [179] for flattened tubes that was analyzed in Shah [154] was not included in the present database. This was because Shah [155] had found that while these

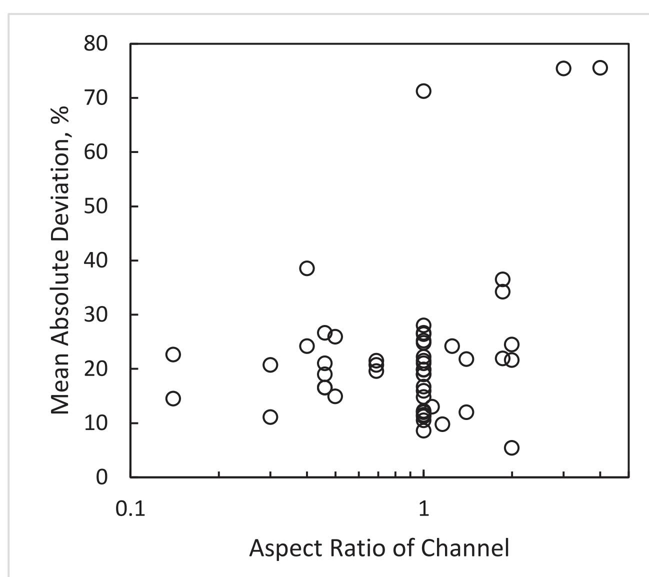

Fig. 5. Effect of channel aspect ratio on MAD of the present correlation with data sets for non-circular channels.

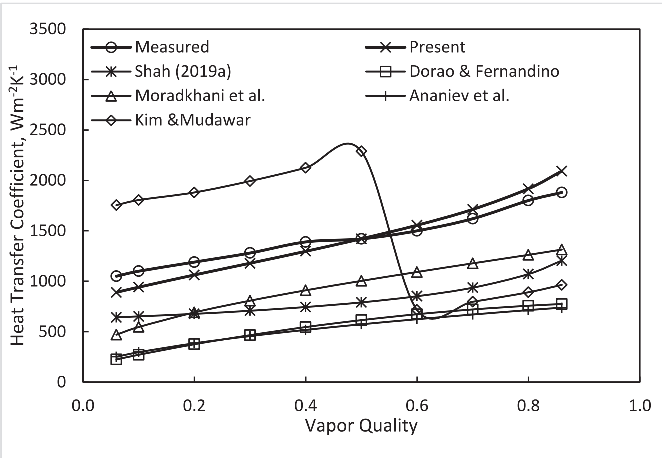

Fig. 6. Data of Son & Lee for R-134a in a horizontal tube compared with various correlations. D = 5.8 mm. T_{SAT} = 40 °C, G = 42 $kgm^{-2}s^{-1}$, We_{GT} = 34, Fr_{LT} = 0.0237. Note the improvement of the present correlation over the Shah [154] correlation.

data for AR up to 14 were in satisfactory agreement with the Shah [154] correlation, some of the data for flattened tubes from other sources were giving large deviations. On the other hand, data for channels other than flattened tubes were giving good agreement. It was therefore decided not to include the data for flattened tubes in the present analysis. Channels made from flattened tubes will be investigated when more data becomes available.

5.5. Effect of froude number

In Shah [154] for horizontal flow, Regimes I and III occur only if $Fr_{LT} > 0.012$, otherwise Regime II occurs. In the present correlation, this limit is set at $Fr_{LT} > 0.026$. An example of the improvement due to this change is seen in Fig. 6 . The present correlation is in good agreement with data while other correlations, including Shah [154], give large deviations.

5.6. Regime III boundary in vertical downflow

As was described in Section 3.1.1, present research showed that besides the condition in Shah [144] correlation for the occurrence of Regime III, it also occurs in vertical downflow if $Re_{LT} < 600$ and $We_{GT} < 100$. The liquid film remains laminar at such low liquid Reynolds number and low vapor shear, thus meeting the conditions assumed by Nusselt in his analysis which led to Eq. (3). This modification resulted in improved agreement with several data sets. For the 43 data points affected by this change, the MAD of the present correlation is 12.3% while that of Shah [154] is 23.6%. The MAD of correlations of others range from 55% to 117%. The improvement is illustrated in Fig. 7 which shows the data of Kurita et al. [99] for FC-72.

5.7. Applicability to various fluid types

Table 6 lists the deviations of the present and other correlations with different types of fluids. These results are discussed in the following.

It is seen that the data for water are from fourteen sources and the present correlation is in good agreement with MAD of 15.9%. Correlations by others all have large deviations ranging from 35% to 65%. An example is seen in Fig. 8 which shows the data of Al-Shammari et al. [6] in a vertical tube. Figs. 9 and 10 show, respectively the data of Caruso et al. [32] and Wang and Du [172] for water in horizontal tubes. Excellent agreement is seen with the

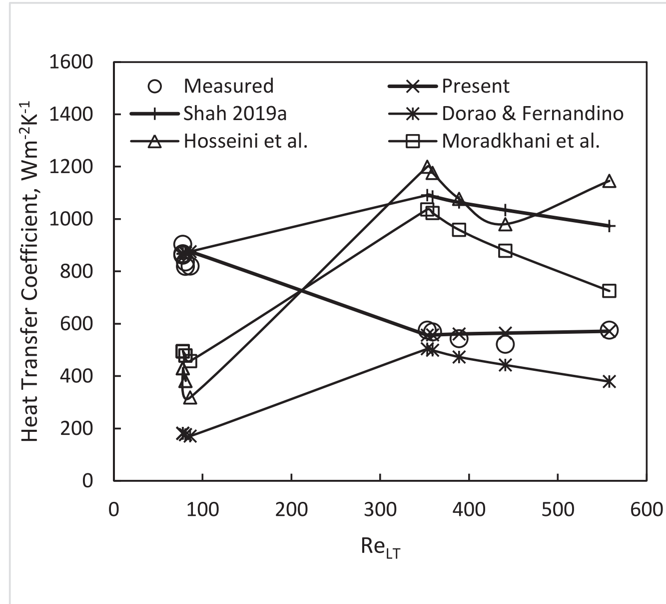

Fig. 7. Mean heat transfer coefficient data of Kurita et al [99] for FC-72 in a vertical tube compared to the present and other correlations. Note the improvement of the present correlation over the Shah (2019) correlation.

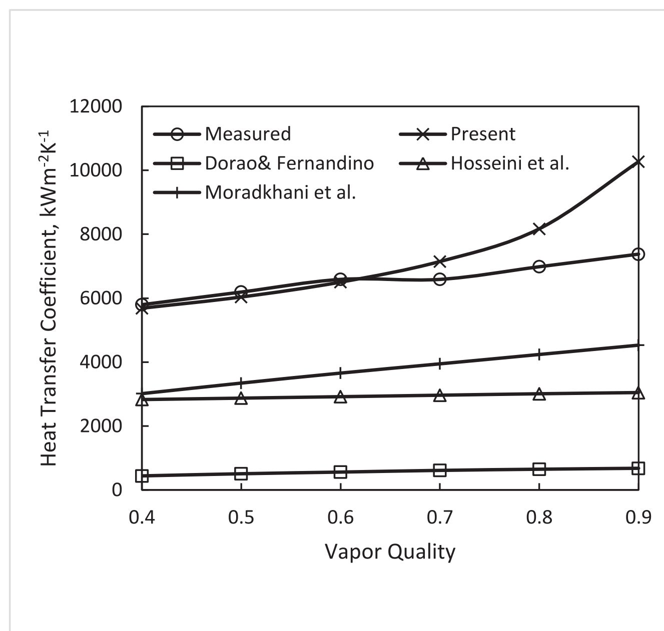

Fig. 8. Comparison of the present and some other correlations with the data of Al-Shammari et al. [6]. Water flowing down in a vertical tube 26.2 mm diameter, G = 3 $kgm^{-2}K^{-1}$, T_{SAT} = 56.5 °C, We_{GT} = 34.

present correlation while all others show large deviations from data. It indicates that the present correlation is the only one which can be relied upon for water.

All correlations show fairly good agreement with data for carbon dioxide. Best agreement is with the present correlation which has MAD of 21.9% while the Kim and Mudawar correlation has MAD of 31.2%.

For the halocarbon refrigerants, the present correlation has the least MAD at 17.5%. The next best correlation is that of Moradkhani et al. with MAD of 20.6%. Most of the correlations give fairly good agreement with halocarbon refrigerant data.

Table 6
Deviation of Correlations with data for various types of fluids.

Fluid	Number of Sources	N	Deviation, %Mean AbsoluteAverage Shah [141]	Shah [144]	Shah [154]	Present	Kim & Mudawar	Ananiev et al.	Dorao & Fer-nandino	Hosseini et al	Moradkhani et al.	Moser et al.	Traviss et al.	Akers et al.
Water	14	333	38.3	17.8	16.0	15.9	38.7	49.3	65.4	43.3	37.3	36.0	84.8	34.8
			-24.5	-2.0	3.6	3.4	4.0	7.2	-64.7	-3.8	-13.3	-26.9	57.1	-16.2
Carbon dioxide	8	346	54.1	23.4	23.3	21.9	31.2	30.1	29.9	28.3	23.7	47.5	168.9	42.9
			32.4	7.9	8.2	3.5	-8.9	-16.9	-12.1	-2.1	-4.2	25.0	161.5	35.1
Hydrocarbons	24	1536	41.4	19.4	18.1	17.2	21.9	19.0	20.7	15.5	16.2	45.2	151.8	49.2
			34.1	12.5	10.1	9.1	-11.3	0.0	-8.2	-7.0	-5.1	41.1	150.8	25.3
Ammonia	1	79	38.2	39.7	34.2	34.2	32.6	41.4	49.2	54.4	24.3	46.9	29.0	54.3
			-33.5	-35.7	-24.0	-24.2	-27.3	-38.3	-47.4	-54.1	-16.2	-45.2	8.5	52.8
Halocarbon refrigerants	108	5580	28.6	20.1	18.0	17.5	27.7	25.9	24.9	31.8	20.6	29.4	85.8	68.2
			2.6	-1.8	-1.3	-2.7	-16.8	-19.5	-18.1	3.2	-4.7	12.0	76.5	49.3
HFE's, FC-72, Dowtherm		179	29.0	23.0	22.7	22.5	22.6	24.4	31.7	36.3	35.5	57.5	51.7	94.3
			-18.2	-9.2	3.4	3.6	-13.5	-11.0	-25.8	-11.3	-3.5	48.9	24.7	83.2

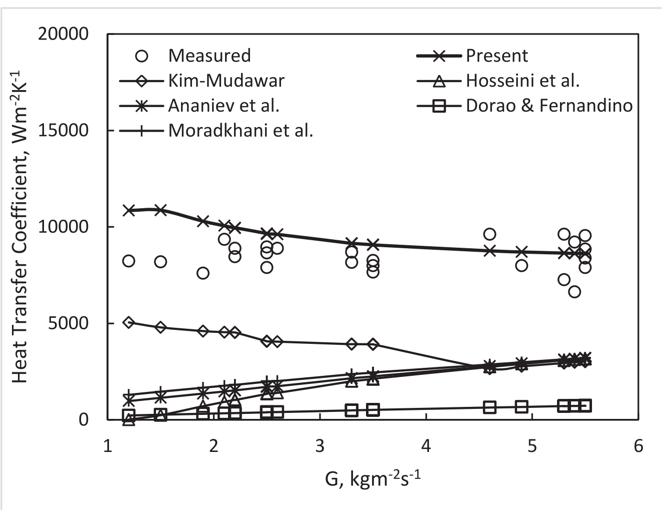

Fig. 9. Mean heat transfer data of Caruso et al. [32] for water condensing in a horizontal tube compared to the present and other correlations. D = 22 mm, T_{SAT} = 100 °C.

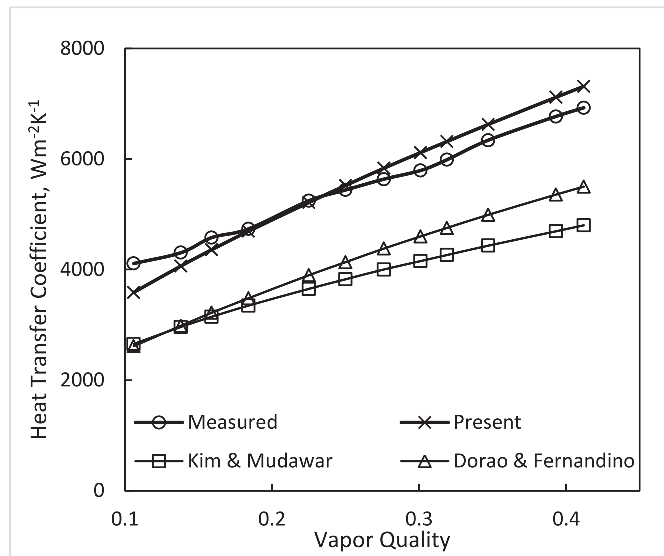

Fig. 11. Comparison of the present and other correlations with the data of Garimella et al. [67] for pentane in a horizontal tube. D = 14.4 mm, T_{SAT} = 74.9 °C, G = 450 $kgm^{-2}K^{-1}$.

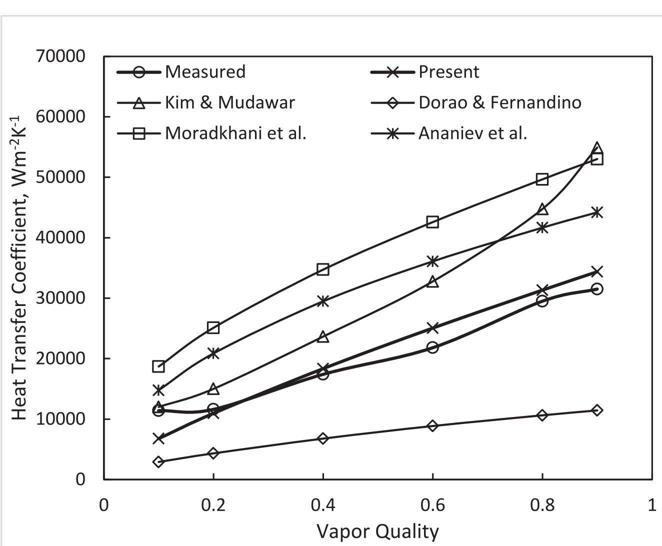

Fig. 10. Comparison of various correlations with water data of Wang and Du [172] in a horizontal tube. D = 2.8 mm, T_{SAT} = 105 °C, G = 65 $kgm^{-2}s^{-1}$.

All correlations are in fairly good agreement with data for hydrocarbons. The MAD of the present correlation is 17.2% while that of Hosseini et al. correlation is the least at 15.5%. Fig. 11 shows the comparison of the present and a couple of other correlations with the data of Garimella et al. [67] for pentane in a horizontal tube.

The agreement of the present correlation with heat transfer fluids (HFE's, FC-72, Dowtherm) is considerably better than the correlations of others. This is seen in Fig. 7 for FC-72, Fig. 12 for Dowtherm, and Fig. 13 for HFE-7100. For these fluids, the MAD of the present correlation is 22.5% while that of others is up to 36.3%.

The only data for ammonia that have been included in the results of the present data analysis are those of Fronk and Garimella [65] in horizontal tubes of diameter 0.98, 1.44, and 2.16 mm. The MAD of the present correlation is 34.2% and AD is -24.2%. Other correlations also predict low, AD being from -16.2% to -54.1%. According to the authors, the maximum uncertainty in the reported heat transfer coefficients is ± 36%. If the reported heat transfer coefficients are reduced by 25%, all correlations will be in adequate agreement with them. Fig. 14 compares data from one of the runs with the present and two other correlations which have performed well with other fluids. Good agreement is seen.

Data from two other experimental studies for ammonia were examined. These are Volrath et al. [171] and Komandiwirya et al.

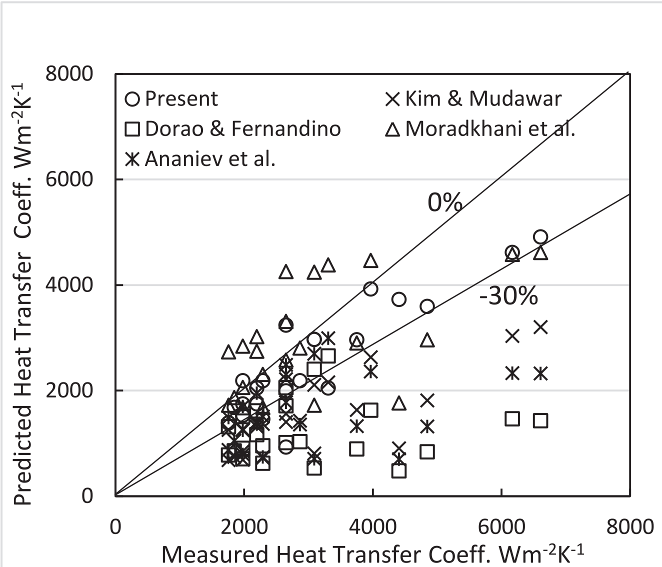

Fig. 12. Comparison of the data of Blangetti and Schulnder [26,27] for Dowtherm 209 in a vertical tube with the present and other correlations. D = 30 mm, T_{SAT} = 97.5 °C.

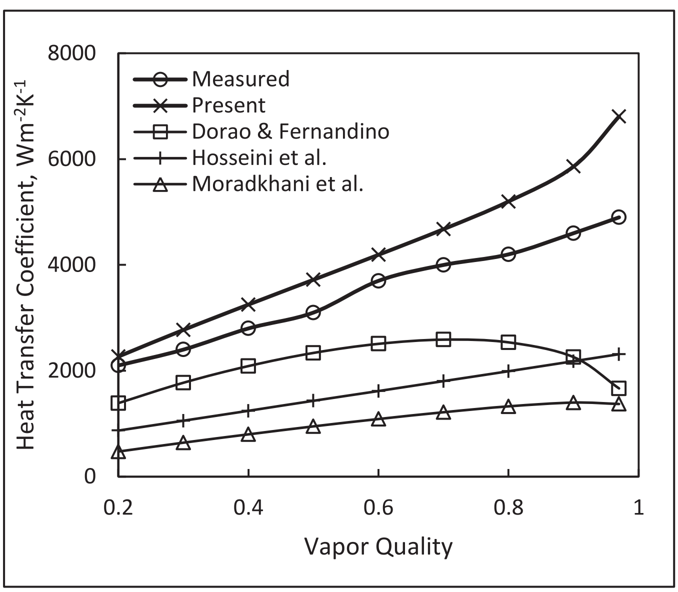

Fig. 13. Comparison of the data of Al-Zaidi et al. [8] for HFE-7100 in a rectangular multichannel with correlations. D_{HYD} = 0.57 mm, D_{HP} = 0.67 mm, T_{SAT} = 60 °C, G = 126 $kgm^{-2}s^{-1}$.

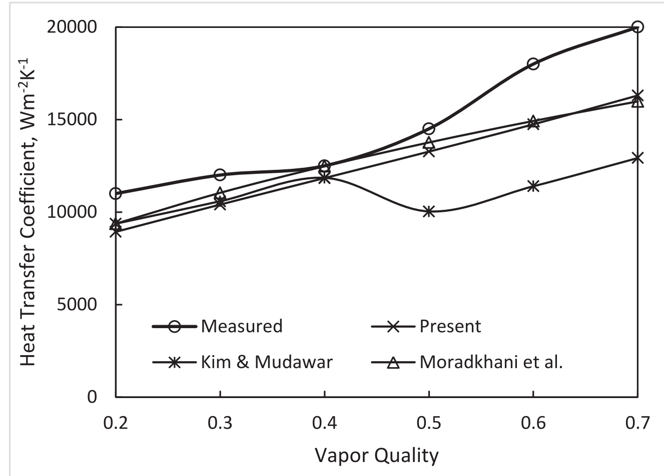

Fig. 14. Data of Fronk and Garimella [65] for ammonia in a horizontal tube compared to present and other correlations. D = 1.44 mm, T_{SAT} = 40 °C, G = 75 $kgm^{-2}s^{-1}$.

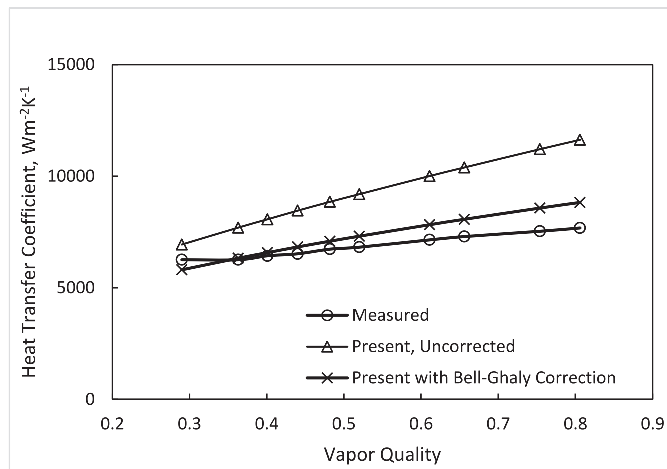

Fig. 15. Comparison of data of Azzolin et al. (2019) for R-455A with the present correlation without correction and with Bell-Ghaly correction for mass transfer effect. D = 0.96 mm, G = 600 $kgm^{-2}s^{-1}$, T_{SAT} = 40 °C, glide = 9.5 K.

[94]. These were done on the same test facility and two of the authors are common to both reports. Hence these should be regarded as a single source. Data from both studies are very low compared to several correlations, for example the well-verified correlation of Cavallini et al. [37] predicts 2 to 3 times the reported heat transfer coefficients.

It may be noted that the data for saturated and subcooled boiling of ammonia in tubes are in excellent agreement with Shah [149,150] general correlations, respectively, which agree well with data for many fluids over very wide ranges. The mechanism of heat transfer during condensation is similar to that during evaporation without bubble nucleation. Therefore, one will not expect heat transfer of condensing ammonia to be different from that of other fluids.

In view of the above discussions, the author feels that the present correlation is suitable for application to ammonia. Further comparison for new data, when available, is needed for confirmation.

5.8. Zeotropic mixtures

The present data analysis included many zeotropic mixtures with glide from 0.1 to 9.5 K. The predictions of all correlations were corrected for mass transfer effects using the Bell and Ghaly [24] method. Fig. 15 shows the effect of this correction on data from a run for R-455A with a glide of 9.5 K. It is seen that this correction brings the predictions of the present correlation in good agreement with the measurements. Similar results were obtained with data for other zeotropic mixtures.

Shah et al. [145] compared an extensive database for condensation of mixtures in tubes with the Shah [143] correlation together with correction factors by Bell and Ghaly [24], McNaught [117] and Del Col et al. [42]. The glide in the data was up to 35.5 K. The MAD using Bell and Ghaly and McNaught methods was about the same. The McNaught method always predicts lower than the Bell-Ghaly method as it assumes an extra resistance due to mass trans-

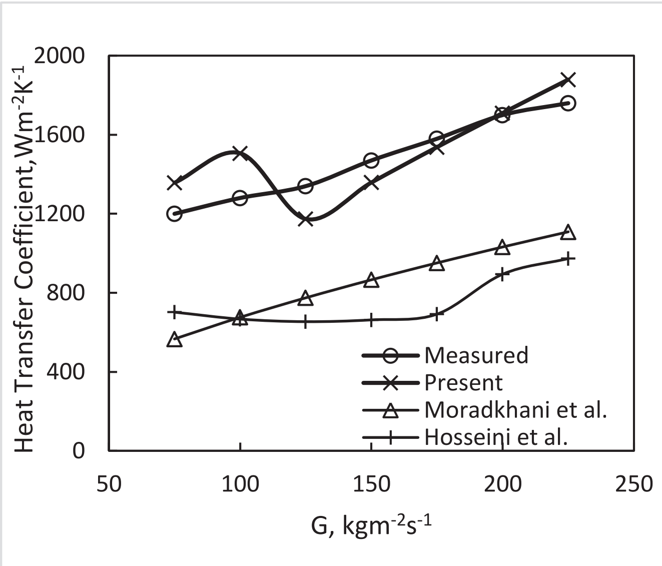

Fig. 16. Comparison of present and other correlations with the mean heat transfer coefficient data of Li et al. [109] in a horizontal annulus. R-410A, T_{SAT} = 45 °C.

fer. MAD using the Del Col et al. factor was higher than with the other two methods.

The Bell and Ghaly method has been found to perform well by many other researchers also. It is therefore recommended.

5.9. Annuli

The data analyzed in Shah [154] did not include any for annuli. Data for annuli from two sources were analyzed during the present research. These are the data of Li et al. [109] for R-410A and those of Borchmann [28] for R-11, both for horizontal annuli.

As seen in Table 1, the data of Li et al. are in good agreement with the present correlation, the MAD being 10.1%. This close agreement is also seen in Fig. 16 . The data of Borchmann [28] have average deviation of -30% and MAD of 30%. These comparatively high deviations are due to heat transfer coefficients being very high near the entrance.

Cavallini et al. [34] condensed R-11 and R-113 in a vertical annulus 38.5 mm OD, 24 mm ID. They report that their data was overpredicted by 20 to 25 % by the Shah [141] correlation. They performed the calculation using D_{HYD} which is 14.5 mm. D_{HP} is 37.8 mm. According to Eq. (7) which is used to calculate single phase heat transfer coefficient, h_{LS} α $D^{-0.2}$. Thus if D_{HP} is used instead of D_{HYD}, heat transfer coefficient will be multiplied by $(14.5/37.8)^{0.2}$ = 0.82. This will bring their data in close agreement with the Shah [141] correlation. As the mass flux is high and pressure low in these data, the predictions of Shah [141] are about the same as those of Shah [144] and hence the present correlation.

The good agreement with the Cavallini et al. data obtained by using D_{HP} confirms that D_{HP} is the correct choice for calculating single phase heat transfer coefficient.

5.10. Applicability range of Shah [141] correlation

Even though improved versions of the Shah correlation have been published, the Shah [141] correlation continues to be widely used in analyzes such as refrigeration systems, heat recovery cycles, and bottoming cycles for power plants. This is probably because of its simplicity and resulting ease of use. To avoid errors due to its use beyond its accurate range, it is desirable to investigate the range in which it could be used with reasonable accuracy.

For all data analyzed, its MAD was found to be 32.9%. The reduced pressure in the data analyzed in Shah [141] was up to 0.44. In Shah [142], the following range of applicability was tentatively suggested; Re_{LT} > 1800, Re_{GT} > 35000, and u_{GT} > 3 ms^{-1}. MAD was calculated for the present database using each of these criteria together with p_r < 0.4. The least MAD was with Re_{GT} < 35000 at 21.7%. With We_{GT} > 100, MAD was 21.5%. For Regime I of the present correlation together with p_r < 0.4, MAD was 20.3%. In any of these conditions, the MAD of the present correlation was around 17%.

Those who use the Shah [141] correlation do so for simplicity. Hence a simple criterion is desirable for them. In view of it, it is recommended to use it only for p_r < 0.4 and We_{GT} >100.

5.11. Recommended range of correlations

As discussed in Section 5.2, all correlations other than the present and Shah [154] have large deviations with horizontal tube data when We_{GT} < 100, for both mini and macro channels. For We_{GT} > 100, Moradkhani et al. correlation has the lowest MAD. However, it gives unsatisfactory agreement with data for water and heat transfer fluids.

In view of the above, the recommendation for horizontal tubes is to use only the present correlation when We_{GT} < 100. The Moradkhani et al. correlation is the best alternative when We_{Gt} > 100 but it should not be used for water and heat transfer fluids (HFE's, FC-72, Dowtherm).

For vertical channels, the MAD of the present correlation is 17.4% while those of other authors are 27.2% to 34.7%. Hence only the present correlation is recommended for vertical tubes.

6. Conclusions

1 A correlation has been presented for condensation in mini and macro channels with horizontal or vertical downflow. It is an improved version of the author's earlier correlation, giving better accuracy.
2 The improved correlation was verified with a database that includes 51 fluids (water, refrigerants, chemicals, cryogens), diameters 0.08 to 49.0 mm, reduced pressures 0.0006 to 0.949, mass flux from 1.1 to 1400 $kgm^{-2}s^{-1}$, various shapes (round, rectangular, triangular, etc.), single and multi-channels, annuli, horizontal and vertical downflow. The improved correlation predicts 8298 data points from 130 sources with mean absolute deviation (MAD) of 17.9 %.
3 The same database was also compared to many other correlations. Their deviations were considerably higher, especially for horizontal channels at We_{GT} < 100, the range in which surface tension effects prevail.
4 Further data analysis is required for ammonia, for hydrocarbons at low We_{GT}, and for annuli to validate and improve this correlation.
5 A simple criteria has been given for determining the reasonably accurate range of the Shah [141] correlation which is widely used in analyses such as refrigeration systems, heat recovery, and bottoming cycles.

Declaration of Competing Interest

The authors declare that they have no known competing financial interests or personal relationships that could have appeared to influence the work reported in this paper.

CRediT authorship contribution statement

Mirza M. Shah: Writing – review & editing, Writing – original draft.

Acknowledgment

This work did not receive financial support from any source.

Reference

[1] H.M. Afroz, A. Miyara, K. Tsubaki, Heat transfer coefficients and pressure drops during in-tube condensation of CO_2/DME mixture refrigerant, Int. J. Refrig. 31 (2008) 1458–1466.
[2] A. Agarwal, T.M. Bandhauer, S. Garimella, Measurement and modeling of condensation heat transfer in non-circular microchannels, Int. J. Refrig. 33 (2010) 1169–1179.
[3] W.W. Akers, H.A. Deans, O.K. Crosser, Condensing heat transfer within horizontal tubes, Chem. Eng. Prog. Symp. Ser. 59 (29) (1959) 171–176.
[4] A. Al-Hajri, A.H. Shoostari, S. Dessiatoun, M.M Ohadi, Performance characterization of R134a and R245fa in a high aspect ratio microchannel condenser, Int. J. Refrig. 36 (2013) 588–600.
[5] E. Allymehr, A.A. Pardinas, T.M. Eikevik, et al., Condensation of hydrocarbons in compact smooth and microfinned tubes, Energies 14 (2021) 2647, doi:10.3390/en14092647.
[6] S.B. Al-Shammari, D.R. Webb, P. Heggs, Condensation of steam with and without the presence of non-condensable gases in a vertical tube, Desalination 169 (2004) 151–160.
[7] M. Altman, F.W. Staub, R.H. Norris, Local heat transfer and pressure drop for Refrigerant 22 condensing in horizontal tubes, in: Proceedings of the ASME AIChE Conference, Storrs, CT, 1959.
[8] A.H. Al-Zaidi, M.M. Mahmoud, T.G. Karayiannis, Condensation flow patterns and heat transfer in horizontal microchannels, Exp.Therm. Fluid Sci. 90 (2018) 153–173.
[9] E.P. Ananiev, I.D. Boyko, G.N. Kruzhilin, Heat transfer in the presence of steam condensation in horizontal tubes, Int. Dev. Heat Transf. 2 (1961) 290–295.
[10] U.C. Andresen, Supercritical gas cooling and near-critical-pressure condensation of refrigerant blends in microchannels, Georgia Institute of Technology, 2007.
[11] C. Aprea, A. Greco, G.P. Vanoli, Condensation heat transfer coefficients for R22 and R407C in gravity driven flow regime within a smooth horizontal tube, Int. J. Refrig. 26 (2003) 393–401.
[12] K. Aroonrat, S. Wongwises, Condensation heat transfer and pressure drop characteristics of R-134a flowing through dimpled tubes with different helical and dimpled pitches, Int. J. Heat Mass Transf. 121 (2018) 620–631.
[13] N.Z. Azer, L.V. Abis, H.M. Soliman, Local heat transfer coefficients during annular flow condensation, ASHRAE Trans. 78 (2) (1972) 135–143.
[14] M. Azzolin, S. Bortolina, L.P.L. Nguyen, P. Lavieilleb, A. Glushchuk, P. Queeckers, M. Miscevic, C.S. Iorioc, D. Del Col, Experimental investigation of in–tube condensation in microgravity, Int. Commun. Heat Mass Transf. 96 (2018) 69–79.
[15] M. Azzolin, A. Berto, S. Bortolin, L. Moro, D. Del Col, Condensation of ternary low GWP zeotropic mixtures inside channels, Int. J. Refrig. 103 (2019) 77–90.
[16] M. Azzolin, S. Bortolin, D. Del Col, Convective condensation at low mass flux: effect of turbulence and tube orientation on the heat transfer, Int. J. Heat Mass Transf. 144 (2019) 118646.
[17] J. Bae, L. Maulbetsch, W.M. Rohsenow, Refrigerant Forced Convection Condensation Inside Horizontal Tubes, Massachusetts Institute of Technology, Cambridge, MA, 1968 Report DSR-79760-59.
[18] J. Bae, L. Maulbetsch, W.M. Rohsenow, Refrigerant Forced Convection Condensation Inside Horizontal Tubes, Massachusetts Institute of Technology, Cambridge, MA, 1969 Report DSR-79760-64.
[19] J.R. Baird, D.F. Fletcher, B.S. Haynes, Local condensation heat transfer rates in fine passages, Int. J. Heat Mass Transf. 46 (23) (2003) 4453–4466.
[20] M.K. Bashar, K. Nakamura, K. Kariya, A. Miyara, Experimental study of condensation heat transfer and pressure drop inside a small diameter microfin and smooth tube at low mass flux condition, Appl. Sci. 8 (2018) 2146, doi:10.3390/app8112146.
[21] W. Baik, R. Yun, In-tube condensation heat transfer characteristics of CO_2 with N_2 at near critical pressure, Int. J. Heat Mass Transf. 144 (2019) 118628.
[22] T.M. Bandhauer, A. Agarwal, S. Garimella, Measurement and modeling of heat transfer in circular microchannels, J. Heat Transf. 128 (10) (2006) 1050–1059.
[23] A.L. Belchí, F.I. Gómez, J.R.G. Cascales, F.V. García, Condensing two-phase pressure drop and heat transfer coefficient of propane in a horizontal multiport mini-channel tube: experimental measurements, Int. J. Refrig. 68 (2016) 59–75.
[24] K.J. Bell, M.A. Ghaly, An approximate generalized design method for multicomponent/partial condenser, AIChE Symp. Ser. 69 (1973) 72–79.
[25] N. Berrada, C. Marviller, A. Bontemps, S. Daudi, Heat transfer in tube condensation of a zeotropic mixture of 23/134a in a horizontal smooth tube, Int. J. Refrig. 19 (7) (1996) 463–472.
[26] F. Blangetti, E.U. Schlunder, Local heat transfer coefficients in condensation in vertical tubes, in: Proceedings of the Sixth International Heat Transfer Conference, Toronto, Canada, 1978, pp. 437–442.
[27] F. Blangetti, E.U. Schlunder, P.J. Marto, P.G. Kroger, Local heat transfer coefficients in film condensation at high Prandtl numbers,, in: Condensation Heat Transfer, American Society of Mechanical Engineers, New York, 1979, pp. 17–25.
[28] J. Borchman, Heat transfer of high velocity vapors condensing in annuli, ASHRAE Trans. 73 (1967) VI.2.1–VI.2.13.
[29] V.M. Borishanskiy, D.I. Volkov, N.I. Ivashenko, G.A. Makarova, Yu Illarionov, T. Vorontsova, L. A, I.A. Alekseyev, N.I. Ivashchenko, O.P. Kretunov, Heat transfer in steam condensing inside vertical pipes and coils, Heat Transf. Sov. Res. 10 (4) (1978) 44–58.
[30] F.G. Carpenter, Heat transfer and pressure drop for condensing pure vapors inside vertical tubes at high vapor velocities, Department of Chemical Engineering, University of Delaware, Newark, DE, 1948.
[31] F.G. Carpenter, A.P. Colburn, The effect of vapor velocity on condensation inside tubes, in: General Discussions on Heat Transfer, Institution of Mechanical Engineers, 1951, pp. 20–26. July 1951.
[32] G. Caruso, F. Gianetti, A. Naviglio, Experimental investigation on pure steam and steam-air mixture condensation inside tubes, Int. J. Heat Mass Transf. 30 (2) (2012) 77–84 2012.
[33] A. Cavallini, R. Zecchin, High velocity condensation of R-11 vapors inside vertical tubes, in: Proceedings of the Studies on Heat Transfer in Refrigeration, Proceeding IIR Commission 2, Trondheim, Norway, 1971, pp. 385–396.
[34] A. Cavallini, S. Frizzeri, L. Rossetto, Condensation of refrigerants inside annuli, in: Proceedings of the International Heat Transfer Conference 7, Munich, Germany, 1982, pp. 45–51, doi:10.1615/IHTC7.360. 1982, 6-10 September.
[35] A. Cavallini, G. Censi, D. Del Col, L. Doretti, G.A. Longo, L. Rossetto, Experimental investigation on condensation heat transfer and pressure drop of new refrigerants (R134a, R125, R32, R410A, R236ea) in a horizontal smooth tube, Int. J. Refrig. 21 (2001) 73–87.
[36] A. Cavallini, D.D. Col, L. Doretti, M. Matkovic, L. Rosetto, C. Zilio, Condensation heat transfer and pressure gradient inside multiport minichannels, Heat Transf. Eng. 26 (3) (2005) 45–55.
[37] A. Cavallini, D. Del Col, L. Doretti, M. Matkovic, L. Rossetto, C. Zilio, Condensation in horizontal smooth tubes: a new heat transfer model for heat exchanger design, Heat Transf. Eng. 27 (8) (2006) 31–38.
[38] A. Cavallini, L. Doretti, M. Matkovic, L. Rossetto, Update on condensation heat transfer and pressure drop inside minichannels, Heat Transf. Eng. 27 (4) (2006) 74–87.
[39] M.S. Chitti, N.K. Anand, An analytical model for local heat transfer coefficients for forced convective condensation inside smooth horizontal tubes, Int. J. Heat Mass Transf. 2 (1995) 615–627.
[40] J.G. Collier, J.R. Thome, Convective Boiling and Condensation, 3rd ed., Oxford University Press, Oxford, UK, 1994.
[41] A.S. Dalkilic, O. Agra, Experimental apparatus for the determination of condensation heat transfer coefficients for R-134a and R-600a flowing insive vertical and horizontal tubes respectively, in: Proceedings of the 2009 ASME Summer Heat Transfer Conference, San Francisco, California, USA, 2009.
[42] D. Del Col, A. Cavallini, J.R. Thome, Condensation of zeotropic mixtures in horizontal tubes: new simplified heat transfer model based on flow regimes, J. Heat Transf. 127 (2005) 221–230.
[43] D. Del Col, D. Torresin, A. Cavallini, Heat transfer and pressure drop during condensation of the low GWP refrigerant R1234yf, Int. J. Refrig. 33 (7) (2010) 1307–1318.
[44] D. Del Col, S. Bortolin, A. Cavallini, M. Matkovic, Effect of cross sectional shape during condensation in a single square minichannel, Int. J. heat Mass Transf. 54 (2011) 3909–3920.
[45] D. Del Col, M. Bortolato, M. Azzolin, S. Bortolin, Effect of inclination during condensation inside a square cross section minichannel, Int. J. Heat Mass Transf. 78 (2014a) 760–777.
[46] D. Del Col, M. Bortalato, S. Bortolin, Comprehensive experimental investigation of two-phase heat transfer and pressure drop with propane in a minichannel, Int. J. Refrig. 47 (2014b) 66–84.
[47] D. Del Col, S. Bortolin, E. Das Riva, Predicting methods and numerical modeling of condensation in microchannels, in: Encyclopedia of Two-Phase Heat Transfer and Fluid Flow II –Special Topics and Applications, 3, World Scientific Publication Co, 2015, pp. 37–84. VolumeSpecial Topics in Condensation.
[48] D. Del Col, M. Bortalato, M. Azzolin, S. Bortolin, Condensation heat transfer and two-phase and two-phase frictional pressure drop in a single minichannel with R1234ze(E) and other refrigerants, Int. J. Refrig. 47 (2015) 66–84.
[49] D. Del Col, M. Azzolin, S. Bortolin, A. Berto, Experimental results and design procedures for minichannel condensers and evaporators using propylene, Int. J. Refrig. 83 (2017) 23–38.
[50] M.M Derby, H.J. Lee, R.C. Craft, G.J. Michnac, Y. Pelesa, M.K. Jense, Exploration of Experimental Techniques to Determine the Condensation Heat Flux in Microchannels and Minichannels, IHTC-14, Washington, DC, 2010 2010.
[51] M. Derby, H.J. Lee, Y. Peles, M.K. Jensen, Condensation heat transfer in square, triangular, and semi-circular mini-channels, Int. J. Heat Mass Transf. 55 (2012) 187–197.
[52] A. Diani, P. Brunello, L. Rossetto, R513A condensation heat transfer inside tubes: microfin tube vs. smooth tube, Int. J. Heat Mass Transf. 152 (2020) 119472.
[53] Y. Ding, L. Jia, Study on flow condensation characteristics of refrigerant R410a in a single rectangular micro-channel, Int. J. Heat Mass Transf. 114 (2017) 125–134.
[54] M.K. Dobson, J.C. Chato, J.P. Wattelet, et al., Heat transfer and flow regimes during condensation in horizontal tubes, ACRC TR-57, Air Conditioning and Refrigeration, Center University of Illinois, Urbana, Illinois, 1994.
[55] M.K. Dobson, J.C. Chato, Condensation in smooth horizontal tubes, J. Heat Transf. 120 (1998) 193–213.
[56] T. Dong, Z. Yang, Measurement and modeling of R141b condensation heat

transfer in silicon rectangular microchannels, J. Micromech. Microeng. 18 (2008) 085012 16pp, doi:10.1088/0960-1317/18/8/085012.
[57] C.A. Dorao, M. Fernandino, Simple and general correlation for heat trans- fer during flow condensation inside plain pipes, Int. J. Heat Mass Transf. 122 (2018) 290–305.
[58] S. Eckels, T.M. Doerr, M.B. Pate, Heat Transfer and Pressure Drop During Condensation and Evaporation of R-134a/Oil Mixtures in Smooth And Micro-Fin Tubes, American Society of Heating, Refrigerating and Air-Conditioning Engineers, Inc., Atlanta, 1993 Final Report, RP-630.
[59] S.J. Eckels, B. Tesene, Forced convective condensation of refrigerants R-502 and R-507 in smooth and enhanced tubes, ASHRAE Transa. 102 (2) (2002) 627–638.
[60] J. El Hajal, J.R. Thome, A. Cavallini, Condensation in horizontal tubes, part I: two-phase flow pattern map, Int. J. Heat Mass Transf. 46 (2003) 3349–3363.
[61] D.R.E. Ewim, J.P. Meyer, S.M.A.N.R. Abadi, Condensation heat transfer coefficients in an inclined smooth tube at low mass fluxes, Int. J. Heat Mass Transf. 123 (2018) 455–467.
[62] S. Fries, S. Skusa, A. Luke, Experimental investigaton of condensation of hydrocarbons inside a mild steel tube, in: Proceedings of the 12th IIR Gustav Lorentzen Natural Working Fluids Conference, Edinburgh, 2016 Paper ID 1179.
[63] S. Fries, S. Skusa, A. Luke, Heat transfer and pressure drop of condensation of hydrocarbons in tubes, Heat Mass Transf. (2018), doi:10.1007/s00231-018-2318-2.
[64] B.M. Fronk, S. Garimella, Measurement of heat transfer and pressure drop during condensation of carbon dioxide in microscale geometries, in: Proceedings of the 14th International Heat Transfer Conference (IHTC14), 2, Washington, DC, 2010, pp. 235–243. Aug. 8–13Condensation, Paper No. IHTC14-22987.
[65] B.M. Fronk, S. Garimella, Condensation of ammonia and high-temperature-glide ammonia/water zeotropic mixtures in minichannels–Part I: measurements, Int. J. Heat Mass Transf. 101 (2016) 1343–1356.
[66] S. Garimella, A. Agarwal, B.M. Fronk, Condensation heat transfer in rectangular microscale geometries, Int. J. Heat Mass Transf. 100 (2016) 98–110.
[67] S. Garimella, J. Milkie, M. Macdonald, Condensation heat transfer and pressure drop of low-pressure hydrocarbons and synthetic refrigerants, Int. J. Heat Mass Transf. 161 (2020) 120295.
[68] G. Ghim, J. Lee, Experimental evaluation of the in-tube condensation heat transfer of pure n-pentane/R245fa and their non-azeotropic mixture as an ORC working fluid, Appl. Therm. Eng. 106 (2016) 753–761.
[69] G. Ghim, J. Lee, Condensation heat transfer of low GWP ORC working fluids in a horizontal smooth tube, Int. J. Heat Mass Transf. 104 (2017) 718–728.
[70] J.H. Goodykoontz, R.G. Dorsch, Local Heat Transfer Coefficients for Condensation of Steam in Vertical Downflow Within a 5/8 Inch Diameter Tube, National Aeronautics and Space Administration, Washington, DC, 1967 TN D-3326.
[71] Q. Guo, M. Li, H. Gu, Condensation heat transfer characteristics of low-GWP refrigerants in a smooth horizontal mini tube, Int. J. Heat Mass Transf. 126 (2018) (2018) 26–38.
[72] M. Hirose, J. Ichinose, N. Inoue, Development of the general correlation for condensation heat transfer and pressure drop inside horizontal 4 mm small–diameter smooth and microfin tubes, Int. J. Refrig. 90 (2018) 238–248.
[73] M.A. Hossain, Y. Onaka, A. Miyara, Experimental study on condensation heat transfer and pressure drop in horizontal plain tubes for R-1234ze(E), R-32, and R-410A, Int. J. Refrig. 35 (2012) 927–938.
[74] X. Huai, S. Koyama, An experimental study of carbon dioxide condensation in mini channels, J. Therm. Sci. 13 (4) (2004) 358–365.
[75] X. Huang, G. Ding, H. Hu, Y. Zhu, H. Peng, Y. Gao, B. Deng, Influence of oil on flow condensation heat transfer of R410A inside 4.18 and 1.6 mm inner diameter horizontal smooth tubes, Int. J. Refrig. 33 (2010) 158–169.
[76] O. Iqbal, P. Bansal, In-tube condensation of CO_2 heat transfer in a horizontal smooth tube, Int. J. Refrig. 35 (2) (2012) 270–277.
[77] C.A. Infante-Ferreira, T.A. Newell, J.C. Chato, X. Nan, R404A condensing under forced flow conditions inside smooth, microfin and cross-hatched tubes, Int. J. Refrig. 26 (2003) 433–441.
[78] T.A. Jacob, E.P. Matty, B.M. Fronk, Experimental investigation of in-tube condensation of low GWP refrigerant R450A using a fiber optic distributed temperature sensor, Int. J. Refrig. 103 (2019) 274–286.
[79] M. Jakob, S. Erck, H. Eck, Forschungsheft, Forschugsheft Geb. Ing. Wes. 3 (1932) 290–295.
[80] E.W. Jassim, T.A. Newell, J.C. Chato, Prediction of two-phase condensation in horizontal tubes using probabilistic flow regime maps, Int. J. Heat Mass Transf. 51 (3-4) (2008) 485–496.
[81] Y. Jiang, S. Garimella, Heat transfer and pressure drop for condensation of R-404A at near critical pressure, ASHRAE Trans. 109 (1) (2003) 677–688.
[82] D. Jige, N. Inoue, S. Koyama, Condensation of refrigerants in a multiport tube with rectangular minichannels, Int. J. Refrig. 67 (2016) 202–213.
[83] D. Jung, K. Song, Y. Cho, S. Kim, Flow condensation of heat transfer coefficients of pure refrigerants, Int. J. Refrig. 26 (2003) 4–11.
[84] D. Jung, Y. Cho, K. Park, Flow condensation heat transfer coefficients of R22, R134a, R407C, and R410A inside plain and microfin tubes, Int. J. Refrig. 27 (2004) 25–32.
[85] S.G. Kandlikar, Fundamental issues related to flow boiling in minichannels and microchannels, Exp. Therm. Fluid Sci. 26 (2–4) (2002) 389–407.
[86] J.W. Kang, T. Han, K. Moriyama, et al., Internal condensation heat transfer in a hydrophobic near-horizontal tube with high pressure and low mass flux, Int. J. Heat Mass Transf. 182 (2022) 122046.
[87] B.L. Keinath, S. Garimella, High-pressure condensing refrigerant flows through microchannels, part ii: heat transfer models, Heat Transf. Eng. (2018), doi:10.1080/01457632.2018.1443258.
[88] K. Keniar, B. El Fil, S. Garimella, A critical review of analytical and numerical models of condensation in microchannels, Int. J. Refrig. 120 (2020) 314–330.
[89] K. Keniar, S. Garimella, Experimental investigation of refrigerant condensation in circular and square micro- and mini- channels, Int. J. Heat Mass Transf. 176 (2021) 121383.
[90] S. Kim, I. Mudawar, Flow condensation in parallel micro-channels – part 2: heat transfer results and correlation technique, Int. J. Heat Mass Transf. 55 (2012) 984–994.
[91] N.H Kim, H.H. Gook, B.M. Lee, Condensation heat transfer and pressure drop of R-404A in 7.0 mm O.D. smooth and microfin tube at low mass fluxes, Int. J. Air Cond. Refrig. 26 (1) (2018) 1850005.
[92] C.H. Kim, N.H. Kim, Condensation heat transfer and pressure drop of low GWP R-404A-alternative refrigerants (R-448A, R-449A, R-455A, R-454C) in a 7.0-mm outer-diameter horizontal microfin tube, Int. J. Refrig. 126 (2021) 181–194.
[93] S. Kim, I. Mudawar, Universal approach to predicting heat transfer coefficient for condensing mini/micro-channel flow, Int. J. Heat Mass Transf. 56 (1–2) (2013) 238–250.
[94] H.B. Komandiwirya, P. Hrnjak, T. Newell, An Experimental Investigation of Pressure Drop and Heat Transfer in an In-Tube Condensation System of Ammonia With and Without Miscible Oil in Smooth and Enhanced Tubes, Air Conditioning and Refrigeration Center, University of Illinois at Urbana-Champaign, 2005 Report ACRC CR-54.
[95] C. Kondou, P. Hrnjak, Heat rejection from R744 flow under uniform temperature cooling in a horizontal smooth tube around the critical point, Int. J. Refrig. 34 (2011) 719–731.
[96] S. Koyama, K. Kuwahara, K. Nakashita, Condensation of refrigerant in a multi-port channel, in: Proceedings of the 1st International Conference on Microchannels and Minichannels, Rochester, NY,USA, 2003, pp. 193–205.
[97] V.I. Kozitskiy, A.P. Klimenko, L.F. Tolubinskaya, V.S. Shevchuk, Heat transfer for condensing mixtures of Freons 12 and 22, Heat Transf. Sov. Res. 6 (3) (1971) 171–175.
[98] S.Z. Kuhn, V.E. Schrock, P.F. Peterson, An investigation of condensation from steam-gas mixtures flowing downwards inside a vertical tube, Nucl. Eng. Des. 177 (1997) 53–69.
[99] J. Kurita, M. Kivisalu, S. Mitra, et al., Experimental results on gravity driven fully condensing flows in vertical tubes, their agreement with theory, and their differences with shear driven flows' boundary-condition sensitivities, Int. J. Heat Mass Transf. 54 (2011) 2932–2951.
[100] A. Lambrecht, L. Liebenberg, A.E. Bergles, J.P. Meyer, Heat transfer performance during condensation inside horizontal smooth, micro-fin, and herringbone tubes, J. Heat Transf. 128 (7) (2006) 691–700.
[101] H. Lee, J. Yoon, J. Kim, P.K. Bansal, Condensing heat transfer and pressure drop characteristics of hydrocarbon refrigerants, Int. J.Heat Mass Transf. 49 (2006) 1922–1927.
[102] K. Lee, M.H Kim, Experimental and empirical study of steam condensation heat transfer with a noncondensable gas in a small-diameter vertical tube, Nucl. Eng., Des. (2008) 207–216.
[103] H. Lee, C. Son, Condensation heat transfer and pressure drop characteristics of R-290, R-600a, R-134a, and R-22 in horizontal tubes, Heat Mass Transf. 46 (2010) 571–584.
[104] B.M. Lee, H.H. Gook, S.B. Lee, et al., Condensation heat transfer and pressure drop of low GWP R-404A alternative refrigerants (R-448A, R-449A, R-455A, R-454C) in a 5.6 mm inner diameter horizontal smooth tube, Int. J. Refrig. 128 (2021) 71–82.
[105] E.W. Lemmon, L. Huber, M.O. McLinden, NIST Reference Fluid Thermodynamic and Transport Properties, NIST, Gaithersburg, MD, 2013 REFPROP Version 9.1.
[106] S. Li, J. Han, G. Su, J. Pan, Condensation heat transfer of R-134a in horizontal straight and helically coiled tube-in-tube heat exchangers, J. Hydrodyn. Ser. B 19 (6) (2007) 677–682.
[107] M. Li, Q. Guo, J. Lv, D. Li, Research on condensation heat transfer characteristics of R447A, R1234ze, R134a and R32 in multi-port micro-channel tubes, Int. J. Heat Mass Transf. 118 (2018) 637–650.
[108] P. Li, J.J. Chen, S. Norris, Flow condensation heat transfer of CO_2 in a horizontal tube at low temperatures, Appl. Therm. Eng. 130 (2018) 561–570 Pages.
[109] W. Li, J. Wang, Y. Guo, et al., Two-phase heat transfer of R410A in annuli outside enhanced tubes with micro-fin and dimple, Int. J. Heat Mass Transf. 175 (2021) 121370.
[110] G.M. Lilburne, D.G. Wood, Condensation inside a vertical tube, in: Proceedings of the Seventh International Heat Transfer Conference, Munich, Germany, 1982, pp. 113–117.
[111] N. Liu, J.M. Li, H.S Wang, Heat transfer and pressure drop during condensation of R152a in circular and square microchannels, Exp. Therm. Fluid Sci. 47 (2013) 60–66.
[112] M. Macdonald, Condensation of pure and zeotropic mixtures of hydrocarbons in smooth horizontal tubes Doctorate Thesis, Georgia Institute of Technology, Georgia, USA, 2015.
[113] M. Macdonald, S. Garimella, Hydrocarbon condensation in horizontal smooth tubes: part II–heat transfer coefficient and pressure drop modeling, Int. J. Heat Mass Transf. 93 (2016) 1248–1261.
[114] M. Matkovic, A. Cavallini, D. Del Col, L. Rossetto, Experimental study on condensation heat transfer inside a circular microchannel, Int. J. Heat Mass Transf. 54 (2009) 2311–2323.

[115] S.M. Mazumdar, H.M.M. Afroz, N.A. Hosain, et al., Study of in-tube condensation heat transfer of zeotropic R32/R1234ze(E) mixture refrigerants, Int. J. Heat Mass Transf. 169 (2021) 120859.
[116] W.H. McAdams, Heat Transmission, 3rd ed., McGraw Hill, New York, 1954.
[117] J.M. McNaught, P.J. Marto, P.G. Kroger, Mass-transfer correction term in design methods for multicomponent/partial condensers, in: Condensation Heat Transfer, American Society of Mechanical Engineers, New York, 1979, pp. 111–118.
[118] R.P. Mendes, D.L. Pottie, C.H. Paula, et al., Experimental study to determine the local condensation heat transfer coefficients for R134a flowing through a 4.8 mm internal diameter smooth horizontal tube, Eng. Térm. (Therm. Eng.) 20 (1) (2021) 26–33.
[119] J.P. Meyer, J. Dirker, O.K Adelaja, Condensation heat transfer in smooth inclined tubes for R134a at different saturation temperatures, Int. J. Heat Mass Transf. 70 (2014) 515–525.
[120] J.P. Meyer, D.R.E. Ewim, Heat transfer coefficients during the condensation of low mass fluxes in smooth horizontal tubes, Int. J. Multiph. Flow 99 (4) (2018) 85–99.
[121] J.A. Milke, Condensation of hydrocarbons and zeotropic hydrocarbon/refrigerant mixtures in horizontal tubes Doctorate Thesis, Mech. Eng. Dept., Georgia Institute of Technology, Georgia, USA, 2014.
[122] B. Mitra, Supercritical gas cooling and condensation of refrigerant R410A at near-critical pressures, Georgia Institute of Technology, Georgia, 2005.
[123] S. Mochizuki, Y. Yagi, R. Tandano, W. Jang, Convective filmwise condensation of nonazeotropic binary mixtures in a vertical tube, J. Heat Transf. 106 (1984) 531–538.
[124] T.A. Moreira, Z.H. Ayub, G. Ribatski, Convective condensation of R600a, R290, R1270 and their zeotropic binary mixtures in horizontal tubes, Int. J. Refrig. 130 (2021) 27–43 International Journal of Refrigeration 130, 27–43.
[125] K.W. Moser, R.L. Webb, B. Na, A new equivalent Reynolds number model for condensation in smooth tubes, J. Heat Transf. 120 (1998) 410–416.
[126] D. Murphy, Condensation heat transfer and pressure drop of propane in vertical minichannels Doctorate Thesis, Georgia Institute of Technology, Georgia, 2014.
[127] K. Nakashita, Study on condensation of pure refrigerant R134a in multi-port extruded tubes Doctoral thesis, University (in Japanese), Kyushu, 2002.
[128] X.H. Nan, C.A. Infante-Ferreira, In-tube evaporation and condensation of natural refrigerant R 290 (propane), in: Proceedings of the Fourth IIR Gustav Lorentzen Conference, 2000.
[129] Z. Nie, Q. Bi, S. Lei, H. Lv, Y. Guo, Experimental study on condensation of high--pressure steam in a horizontal tube with pool boiling outside, Int. J. Heat Mass Transf. 108 (2017) 2523–2533.
[130] S. Oh, Experimental and analytical study of the effects of noncondensable gas in a passive condenser system Ph.D. thesis, School of Nuclear Engineering, Purdue University, 2004.
[131] K. Park, D. Jung, T. Seo, Flow condensation heat transfer characteristics of hydrocarbon refrigerants and dimethyl ether inside a horizontal plain tube, Int. J. Multiph. Flow 34 (2008) 628–635.
[132] C.K. Powell, Condensation inside a horizontal tube with high vapor velocity Master's thesis, Department of Mechanical Engineering, Purdue University, West Lafayette, IN, 1961.
[133] A. Pusey, D. Kwack, H. Kim, Heat transfer coefficient and cross-sectional flow structure in condensation of steam in an inclined tube at a low mass flux, Exp. Therm. Fluid Sci. 127 (2021) 110414.
[134] C. Qi, X. Chen, W. Wang, et al., Experimental investigation on flow condensation heat transfer and pressure drop of nitrogen in horizontal tubes, Int. J. Heat Mass Transf. 132 (2019) 985–996.
[135] C. Qi, X. Chen, W. Wang, et al., Experiment and simulation on downward flow condensation of nitrogen in vertical tubes, Int. J. Heat Mass Transf. 146 (2020) 118827.
[136] M.M. Rahman, K. Kariya, A. Miyara, An experimental study and development of new correlation for condensation heat transfer coefficient of refrigerant inside a multiport minichannel with and without fins, Int. J. Heat Mass Transf. 116 (2018) 50–60.
[137] V. Rifert, V. Sereda, V. Gorin, et al., Heat transfer during film condensation inside plain tubes. Review of experimental research, Heat Mass Transf. 56 (2020) 691–713, doi:10.1007/s00231-019-02744-5.
[138] W.M. Rohsenow, J.H. Weber, A.T. Ling, Effect of vapor velocity on laminar and turbulent film condensation, Trans. ASME 78 (8) (1956) 1637–1643.
[139] A. Sarmadian, M. Shahafaee, H. Mashouf, S.G Mohseni, Condensation heat transfer and pressure drop characteristics of R-600a in horizontal smooth and helically dimpled tubes, Exp. Therm. Fluid Sci. 86 (2017) 54–62.
[140] M.M. Shah, A new correlation for heat transfer during boiling flow through pipes, ASHRAE Trans. 82 (2) (1976) 66–86.
[141] M.M. Shah, A general correlation for heat transfer during film condensation inside pipes, Int. J. Heat Mass Transf. 22 (1979) 547–556.
[142] M.M. Shah, Heat transfer during film condensation in tubes and annuli, a literature survey, ASHRAE Trans. 87 (1) (1981) 1086–1105.
[143] M.M. Shah, An improved and extended general correlation for heat transfer during condensation in plain tubes, HVAC&R Res. 15 (5) (2009) 889–913.
[144] M.M Shah, General correlation for heat transfer during condensation in plain tubes: further development and verification, ASHRAE Trans. 119 (2) (2013) 3–11.
[145] M.M. Shah, A.M. Mahmoud, J. Lee, An assessment of some predictive methods for in-tube condensation heat transfer of refrigerant mixtures, ASHRAE Trans. 119 (2) (2013) 38–51.
[146] M.M. Shah, A new flow pattern based general correlation for heat transfer during condensation in horizontal tubes, in: Proceedings of the 15th International Heat Transfer Conference IHTC-15, Kyoto, 2014.
[147] M.M. Shah, A new correlation for heat transfer during condensation in horizontal mini/micro channels, Int. J. Refrig. 64 (2016) 187–202.
[148] M.M. Shah, Comprehensive correlations for heat transfer during condensation in conventional and mini/micro channels in all orientations, Int. J. Refrig. 67 (2016) 22–41.
[149] M.M. Shah, Unified correlation for heat transfer during boiling in plain mini/micro and conventional channels, Int. J. Refrig. 74 (2017) 604–624.
[150] M.M. Shah, New correlation for heat transfer during subcooled boiling in plain channels and annuli, Inte. J. Therm. Sci. 112 (2017) 358–370.
[151] M.M. Shah, Applicability of correlations for boiling/condensing in macrochannels to minichannels, Heat Mass Transf. Res. J. 2 (1) (2018) 22–32.
[152] M.M. Shah, Improved general correlation for heat transfer during gas-liquid flow in horizontal tubes, J. Therm. Sci. Eng. Appl. 10 (2018) 051009 -1 to 7.
[153] M.M. Shah, General correlation for heat transfer to gas-liquid flow in vertical channels, J. Therm. Sci. Eng. Appl. 10 (2018) 061006 -1 to 9.
[154] M.M. Shah, Improved correlation for heat transfer during condensation in conventional and mini/micro channels, Int. J. Refrig. 98 (2019) 222–237.
[155] M.M. Shah, Prediction of heat transfer during condensation in non-circular channels, Inventions 4 (2019) 31, doi:10.3390/inventions4020031.
[156] M.M. Shah, Two-Phase Heat Transfer, John Wiley & Sons, 2021.
[157] S. Shen, Y. Wang, D. Yuan, Circumferential distribution of local heat transfer coefficient during steam stratified flow condensation in vacuum horizontal tube, Int. J. Heat Mass Transf. 114 (2017) 816–825.
[158] D.W. Shao, E. Granryd, Heat transfer and pressure drop of HFC134a-oil mixtures in horizontal condensing tube, Int. J. Refrig. 18 (8) (1995) 524–533.
[159] J.S. Shin, M.H Kim, An experimental study of flow condensation heat transfer inside circular and rectangular mini-channels, in: Proceedings of the 2nd International Conference on Microchannels and Minichannels, Rochester, NY, USA, 2004, pp. 633–640.
[160] A.K. Solanki, R. Kumar, Condensation of R-134a inside micro-fin helical coiled tube-in-shell type heat exchanger, Exp. Therm. Fluid Sci. 93 (2018) 344–355.
[161] C. Son, H. Lee, Condensation heat transfer characteristics of R-22, R-134a and R-410A in small diameter tubes, Heat Mass Transf. 45 (2009) 1153–1166.
[162] S. Sung-Hoon, Y. Jung-In, L. Joon_Hyuk, et al., Condensation heat transfer characteristics of R-1234yf with the variation of tube diameter, J. Korean Sol. Energy Soc. 41 (4) (2021) 161–171.
[163] L. Tang, M.M. Ohadi, A.T. Johnson, Flow condensation in smooth and micro-fin tubes with HCFC-22, -134a and -410A refrigerants, Enhanc. Heat Transf. 7 (2000) 289–310.
[164] J.B. Tepe, A.C. Mueller, Condensation and subcooling inside an inclined tube, Chem. Eng. Prog. 43 (5) (1947) 267–278.
[165] W. Tang, T.A. Khan, B. Zheng, et al., Effects of materials on the heat transfer coefficient during condensation and evaporation of R410A, J. Sol. Energy Eng. 143 (2021) 031007 -1-10.
[166] P. Toninelli, S. Bortolin, M. Azzolin, D. Del Col, Effects of geometry and fluid properties during condensation in minichannels: experiments and simulations, Heat Mass Transf. 55 (1) (2019) 41–57.
[167] D. Traviss, W. Rohsenow, A. Baron, Forced-convection condensation inside tubes: a heat transfer equation for condenser design, ASHRAE Trans. 79 (1) (1973) 157–165.
[168] A. Vardhan, Master of Science in Mechanical Engineering Thesis, University of Illinois in Urbana-Champagne, 1997.
[169] V.C. Varma, Master of Science Thesis, Department of Mechanical Engineering, Rutgers University, New Brunswick, NJ, 1977.
[170] V. Vins, A. Aminian, D. Celny, et al., Surface tension and density of dielectric heat transfer fluids of HFE type-experimental data at 0.1 MPa and modeling with PC-SAFT equation of state and density gradient theory, Int. J. Refrig. 131 (2021) 956–969.
[171] J.E. Vollrath, P. Hrnjak, T. Newell, An Experimental Investigation of Pressure Drop and Heat Transfer in an In-Tube Condensation System of Pure Ammonia, Air Conditioning and Refrigeration Center, University of Illinois at Urbana-Champaign, 2003 Report ACRC CR-51.
[172] B.X. Wang, X.Z. Du, Study on laminar film-wise condensation for vapor flow in an inclined small/mini-diameter tube, Int. J. Heat Mass Transf. 43 (2000) 1859–1868.
[173] X,W. Wang, J.Y. Ho, K.C. Leong, et al., Condensation heat transfer and pressure drop characteristics of R-134a in horizontal smooth tubes and enhanced tubes fabricated by selective laser melting, Int. J. Heat Mass Transf. 126 (2018) 949–962.
[174] L. Wang, P. Jio, C. Dang, et al., Condensation heat and mass transfer characteristics of low GWP zeotropic refrigerant mixture R1234yf/R32 inside a horizontal smooth tube: an experimental study and non-equilibrium film model development, Int. J. Therm. Sci. 170 (2021) 107090.
[175] H.S. Wang, J.W, Rose, A theory of film condensation in horizontal noncircular section microchannels, ASME J. Heat Transf. 127 (10) (2005) 1096–1105.
[176] H.S. Wang, J.W. Rose, Theory of heat transfer during condensation in microchannels, Int. J. Heat Mass Transf. 54 (11–12) (2011) 2525–2534.
[177] M. Wen, C. Ho, J. Hsieh, Condensation heat transfer and pressure drop characteristics of R-290 (propane), R-600 (butane), and a mixture of R-290/R-600 in the serpentine small-tube bank, Appl. Therm. Eng. 26 (2006) 2045–2053.
[178] H. Wijaya, M.W. Spatz, Two-phase flow heat transfer and pressure drop characteristics of R-22 and R-32/R125, ASHRAE Trans. 101 (1) (1995) 1020–1027.

[179] M.J. Wilson, T.A. Newell, J.C. Chato, C.A. Infante Ferreira, Refrigerant charge, pressure drop, and condensation heat transfer in flattened tubes, Int. J. Refrig. 26 (2003) 443–451.
[180] Z. Wu, B. Sunden, L. Wang, W. Li, Convective condensation inside horizontal smooth and microfin tubes, J. Heat Transf. 136 (2014) 051504 -1 to 11.
[181] F. Xing, J. Xu, J. Xie, H. Liu, Z. Wang, X. Ma, Froude number dominates condensation heat transfer of R245fa in tubes: effect of inclination angles, Int. J. Multiph. Flow 71 (2015) 98–115.
[182] .Y.Y. Yan, T.F. Lin, Condensation heat transfer and pressure drop of refrigerant R-134a in a small pipe, Int. J. Heat Mass Transf. 42 (1999) 697–708.
[183] J. Yu, J. Chen, F. Li, W. Ca, L. Lu, Y. Jiang, Experimental investigation of forced convective condensation heat transfer of hydrocarbon refrigerant in a helical tube, Appl. Therm. Eng. 129 (2018) 1634–1644.
[184] H. Zhang, X. Fang, H. Shang, W. Chen, Flow condensation heat transfer correlations in horizontal channels, Int. J. Refrig. 59 (2015) 102–114.
[185] B. Zheng, J. Wang, Y. Guo, et al., An experimental study of in-tube condensation and evaporation using enhanced heat transfer (EHT) tubes, Energies 14 (2021) 867, doi:10.3390/en14040867.
[186] X.R. Zhuang, M.Q. Gong, X. Zou, G.F. Chen, J.F. Wu, Experimental investigation on flow condensation heat transfer and pressure drop of R170 in a horizontal tube, Int. J. Refrig. 66 (2016) 105–120 .A.
[187] X.R. Zhuang, G.F. Chen, X. Zou, Q.L. Song, M.Q. Gong, Experimental investigation on flow condensation of methane in a horizontal smooth tube, Int. J. Refrig. 78 (2017) 193–214.
[188] J. Zilly, J. Jang, P. Hrnjak, Condensation of CO_2 at Low Temperature Inside Horizontal Micro-Finned Tube, University of Illinois at Urbana Champaign, 2003 ACRC Report CR-49.
[189] B. Ghorbani, M.A. Akhavan-Behabadib, S. Ebrahimi, K. Vijayaraghavan, Experimental investigation of condensation heat transfer of R600a/POE/CuO nano-refrigerant in flattened tubes, International Communications in Heat and Mass Transfer 88 (2017) 236–244.
[190] S.H. Hosseini, M.A. Moradkhani, M. Valizadeh, A. Zendehboudi, M. Olazar, A general heat transfer correlation for flow condensation in single port mini and macro channels using genetic programming, Int. J. Refrig. 119 (2020) 376–389.
[191] M.A. Moradkhani, S.H. Hosseini, Mengjie Song, Robust and general predictive models for condensation heat transfer inside conventional and mini/micro channel heat exchangers, Applied Thermal Engineering 201 (2022) 117737 Part A.
[192] B. Ren, L. Zhang, H. Xu, J. Cao, Z. Tao, Experimental study on condensation of steam/air mixture in a horizontal tube, Experimental Thermal and Fluid Science 58 (2014) 145–155.

Further reading

[193] S. Kim, I. Mudawar, Theoretical model for annular flow condensation in rectangular micro-channels, Int. J. Heat Mass Transf. 55 (2012) 958–970.